SANDIA REPORT

SAND2013-0743
Unlimited Release
Printed February 2013

Radiobiological Studies Using Gamma and X Rays

Charles A. Potter, Susan W. Longley, Bobby R. Scott, Yong Lin, Julie A. Wilder, Julie A. Hutt, Mabel T. Padilla, and Katherine M. Gott

Prepared by
Sandia National Laboratories
Albuquerque, New Mexico 87185 and Livermore, California 94550

Sandia National Laboratories is a multi-program laboratory managed and operated by Sandia Corporation, a wholly owned subsidiary of Lockheed Martin Corporation, for the U.S. Department of Energy's National Nuclear Security Administration under contract DE-AC04-94AL85000.

Approved for public release; further dissemination unlimited.

Sandia National Laboratories

Issued by Sandia National Laboratories, operated for the United States Department of Energy by Sandia Corporation.

NOTICE: This report was prepared as an account of work sponsored by an agency of the United States Government. Neither the United States Government, nor any agency thereof, nor any of their employees, nor any of their contractors, subcontractors, or their employees, make any warranty, express or implied, or assume any legal liability or responsibility for the accuracy, completeness, or usefulness of any information, apparatus, product, or process disclosed, or represent that its use would not infringe privately owned rights. Reference herein to any specific commercial product, process, or service by trade name, trademark, manufacturer, or otherwise, does not necessarily constitute or imply its endorsement, recommendation, or favoring by the United States Government, any agency thereof, or any of their contractors or subcontractors. The views and opinions expressed herein do not necessarily state or reflect those of the United States Government, any agency thereof, or any of their contractors.

Printed in the United States of America. This report has been reproduced directly from the best available copy.

Available to DOE and DOE contractors from
U.S. Department of Energy
Office of Scientific and Technical Information
P.O. Box 62
Oak Ridge, TN 37831

Telephone: (865) 576-8401
Facsimile: (865) 576-5728
E-Mail: reports@adonis.osti.gov
Online ordering: http://www.osti.gov/bridge

Available to the public from
U.S. Department of Commerce
National Technical Information Service
5285 Port Royal Rd
Springfield, VA 22161

Telephone: (800) 553-6847
Facsimile: (703) 605-6900
E-Mail: orders@ntis.fedworld.gov
Online ordering: http://www.ntis.gov/help/ordermethods.asp?loc=7-4-0#online

SAND2013-0743
Unlimited Release
Printed February 2013

Radiobiological Studies Using Gamma and X Rays

Charles A. Potter
National Security Studies Department
Sandia National Laboratories
P.O. Box 5800
Albuquerque, NM 87185-0425
capotte@sandia.gov

Susan W. Longley
Policy and Decision Analytics
Sandia National Laboratories
P.O. Box 5800
Albuquerque, NM 87185-0425
swlongl@sandia.gov

Bobby R. Scott,
Yong Lin,
Julie A. Wilder,
Julie A. Hutt,
Mabel T. Padilla, and
Katherine M. Gott
Lovelace Respiratory Research Institute
2425 Ridgecrest Drive Southeast
Albuquerque, NM 87108 bscott@lrri.com

Abstract

There are approximately 500 self-shielded research irradiators used in various facilities throughout the U.S. These facilities use radioactive sources containing either ^{137}Cs or ^{60}Co for a variety of biological investigations. A report from the National Academy of Sciences[1] described the issues with security of particular radiation sources and the desire for their replacement. The participants in this effort prepared two peer-reviewed publications to document the results of radiobiological studies performed using photons from 320-kV x rays and ^{137}Cs on cell cultures and mice. The effectiveness of X rays was shown to vary with cell type.

Acknowledgment

We would like to express our appreciation to the U. S. Department of Energy, NA-22, Radiation Source Replacement Program and Frances Keel (DOE/NA-221) for supporting this joint research between Sandia National Laboratories and LRRI. In addition, Philip Rivera in SNL's property management group was instrumental in determining the final disposition of the XRAD-320 used in this work. The LRRI participants are especially grateful to Susan Longley, Gus Potter, and Cody Steel of Sandia and to Dave Griego, Loraine Vigil, Martha Vigil, Isela Parsonese, and Catherine Lambert of LRRI for their assistance in the project.

Contents

Acronyms **6**

1 Introduction **7**

Irradiators 8

Gammacell 1000 Unit 8

X-RAD 320 Unit 9

Summary of LRRI Cell Culture Studies 9

Summary of LRRI Mouse Studies 11

Needed Follow-On Studies 13

Other Radiobiological Studies that Could Be Carried Out Using an X-RAD 320 Unit or a Cesium-137 Unit 14

2 Issues Related to Replacing Cs-137 Sources with X-ray Units **15**

3 Deliverables **17**

References **18**

Appendix

A Biological Microdosimetry Based on Radiation Cytotoxicity Data **21**

B A Comparison of In Vivo Cellular Response to Cs-137 Gamma rays and 320 kV X Rays **31**

Acronyms

ATM Ataxia telangiectasia mutated (DNA damage-responding factor)

BMT Bone marrow transplantation

CNS Central nervous system

DNA Deoxyribonucleic acid

DOE United States Department of Energy

GVHD Graft-versus-host disease

HBEC Human bronchial epithelial cell

HeLa ("Henrietta Lacks") cervical cancer cell line

HFL Human lung fibroblast

HVL Half value layer

LRRI Lovelace Respiratory Research Institute

MCF-7 ("Michigan Cancer Foundation") breast cancer cell line

MHC Major histocompatibility complex

MTT Assay Microculture tetrazolium assay

RBE Relative biological effectiveness

Chapter 1

Introduction

Self-shielded cesium-137 chloride (^{137}CsCl) irradiators with radioactivity levels in the International Atomic Energy Agency Categories 1 and 2 (i.e., greater than 27 Ci) are widely used in three major applications[2]: (1) blood sterilization, (2) radiobiological research involving cells in culture and small animals, and (3) calibration. Cesium-137 was selected because of the radiological properties of ^{137}Cs, including its desirable single (662 keV, for unshielded photons) energy spectrum, long half-life, relative low cost, and moderate shielding requirements relative to some other radionuclides. In the ^{137}Cs irradiators, the ^{137}CsCl which is in a compressed power form is doubly-encapsulated in stainless steel capsule.[2] The physical form is used because of its high specific activity (gamma-ray emissions per unit volume) and manufacturability. The energy spectrum is distorted by the encapsulation.

Cesium chloride is highly soluble in water and is dispersible in aerosol form (e.g., dirty bomb). This has raised homeland security concerns[2] as ^{137}CsCl could be used by terrorists if acquired. Because of this concern, a report by the National Research Council[1] recommended that careful consideration be given to the possibility of replacing ^{137}Cs irradiators with X-ray irradiators.

Whereas unshielded ^{137}Cs-generated gamma rays have an energy of 662 keV, X rays generated from cabinet irradiators typically have photon energies (variable) <500 keV, thus, potentially limiting their ability to penetrate tissues. A recent dosimetric study conducted by Sandia National Laboratories for the Domestic Nuclear Detection Office of the U.S. Department of Homeland Security compared the current line of X-ray research irradiators to several commonly used ^{137}CsCl irradiators and suggested that the X-ray irradiators provided equivalent performance in terms of dose rate, irradiation field size, and uniformity over the field.[3] In addition, the depth-dose for the 320-kV X-ray spectrum was nearly identical to that of ^{137}CsCl down to a depth in tissue of 4 cm).[3]

Research reported here relates to possibly replacing ^{137}CsCl irradiators used in radiobiological research involving cells in culture and small animals with an X-RAD 320 Unit (X-ray source[4]) with energies higher than for a typical X-ray irradiator. The objective of this research was to demonstrate the feasibility of achieving the same success in radiobiological research using the X-ray source as is achieved with higher energy gamma rays from a ^{137}CsCl source. In addition to this report, the required deliverables were two peer-reviewed articles, included as Appendices A and B. It was found that the effectiveness of X rays compared to ^{137}Cs gammas is dependent on cell type. Maintenance issues became evident, such as the heat load of the X-RAD 320 causing a need

Figure 1.1. Gammacell® 1000 Unit[5]

to improve the air conditioning system in the room in which it was installed.

Irradiators

Gammacell 1000 Unit

The Gammacell®[1] 1000 unit[5] (Fig. 1.1) used at Lovelace Respiratory Research Institute (LRRI) is a self-contained irradiator that was designed to deliver large radiation doses to small

[1] Best® Theratronics, Springfield, VA

biological samples. The irradiator consists of a stationary ^{137}Cs doubly-encapsulated radiation source permanently secured within a biological shield. The biological shield is mounted on a steel frame and covered with sheet-metal panels.

The biological shield contains the sample chamber rotor. By turning the rotor through an arc of up to 180 degrees, the sample chamber is either exposed to or removed (except for leakage radiation) from the radiation field and the irradiated target can be rotated during irradiation. The rotor is driven by an electrical drive assembly that is mounted on top of the biological shield. The control panel is located at the top of the unit's front face (Fig. 1.1). The radioactive source is stationary and permanently housed within the stator section of the biological shield. The radioactive source consists of an array of two ^{137}CsCl pencils (Model ISO-1000[5]). The radiation beam is horizontal. The Gammacell® 1000 Unit is housed in a highly secure area at LRRI.

X-RAD 320 Unit

The X-RAD 320 Unit[4] (Fig. 1.2) used at LRRI is a self-contained X-ray irradiation system that was designed for use in biology and medical research. The X-RAD 320 Irradiation System is used in conjunction with the GE ISOVOLT 320 TITAN[2] X-ray unit. A Cathode Generator with a Power Electronics Module and Anode Generator are used to generate the negative and positive high voltages used to excite the X-ray tube. Cooling is achieved via an oil-to-air cooling system.

The shielded cabinet includes an Adjustable Specimen Shelf, Sample Viewing Window and Beam Hardening Filter Holder. The TouchRAD Control Panel is a multi-user, password protected touch-screen interface with a transportable database that can track individual system usage. Passwords, programmed exposure settings, and database management are under the control of a super-user.

The 320 kV X-ray tube provides a high output relatively uniform vertical beam with a maximum output of 4000 watts allowing for delivery of up to 16 Gy/min at 50 cm source to surface distance (SSD). Actual dose rates depend on other factors including beam filtration and other exposure settings. Two filters have been employed in our research: Filter #1, 2.0 mm aluminum (half value layer $\cong$ 1.0 mm Cu) and Filter #2, comprised of 0.75 mm tin + 0.25 mm copper + 1.5 mm aluminum (half value layer $\cong$ 3.7 mm Cu). The unit is also housed in a secure area at LRRI.

Summary of LRRI Cell Culture Studies

Cell cultures studies were conducted using several human cell lines (normal and cancer cells) and several nonzero radiation doses along with unirradiated controls. X-ray doses were assigned based on an initial RBE estimate of 1.3 relative to ^{137}Cs gamma rays. Well-defined, dose-response relationships were achieved using two lines of normal bronchial epithelial cells (HBEC-2 and

[2]General Electric Company, Schenectady, NY

Figure 1.2. X-RAD 320 biological irradiator[4]. Cathode Generator with Power Electronics Module not shown.

HBEC-13) and a line of lung fibroblast (HFL-1). Well-defined, dose-response relationships were also achieved for three cancer cell lines: (1) a lung cancer cell line (A549); (2) a cervical cancer cell line (HeLa); and (3) a breast cancer cell line (MCF-7).

Assays employed that yielded useful dose-response relationships for the range of doses studied were as follows: (1) The Western Blot Assay, (2) the MTT Assay (a colorimetric assay), (3) the Cell Migration Assay, and (4) the Colony Formation Assay.

The widely-used Western Blot Assay, which measures protein expression levels and protein modifications (i.e., phosphorylation) in response to cellular damage, was used to monitor cellular (HBEC-2 cell line) responses to radiation-induced DNA damage. Proteins monitored and yielding well-defined dose-response relationships were DNA damage-responding factors Ataxia telangiectasia mutated (ATM), p53, and p21. Similar dose-response relationships were obtained for X-ray and gamma-ray exposures.

The widely-used MTT assay, which is a metabolic-activity-status assay, was used to measure cytotoxicity for X-ray and gamma-ray exposure of the indicated normal and cancer cell lines. Dose-response relationships obtained were similar for both radiation sources. A *biological-microdosimetry-based, dose-response model for cytotoxicity* was used to evaluate the X-ray RBE for cytotoxicity relative to gamma rays. The X-ray RBE estimates (central) for cytotoxicity for normal cells ranged from 1.5 for HBEC-13 cells to 1.6 for HBEC-2 cells, for the X-ray Filter #1 with half value layer (HVL) $\cong$ 1.0 mm Cu. The X-ray RBE estimates (central) for cytotoxicity for cancer cells ranged from 1.2 for HeLa cells to 1.5 for A549 cells, for the X-ray Filter #2 with HVL $\cong$ 3.7 mm Cu. Attachment 1 provides a paper[6] that was published in Radiation Protection Dosimetry that details the cytotoxicity studies.

The widely-used Cell Migration Assay was employed for HeLa and A549 cancer cells. High migration and invasion capacity is a property of cancer cells. Similar cell migration dose-response relationships were obtained after X-ray (Filter #2) and gamma-ray exposures.

The widely-used Colony Formation Assay was also employed for the A549 cancer cells. The assay measures cell killing and can be used in neoplastic transformation studies involving normal cells. Similar dose-response relationships were obtained after X-ray (Filter #2) and gamma-ray exposures.

Table 1.1 summarizes the assays employed using normal and cancer cell lines and whether or not similar dose-response relationships were achieved using X-rays from the X-RAD 320 Unit as were obtained using the ^{137}Cs source (Gammacell® 1000 Unit).

Summary of LRRI Mouse Studies

Bone marrow transplantation (BMT) after bone marrow ablation during high-dose radiation therapy is one possible approach for treating leukemia, some solid tumors, and some metabolic diseases. The field of BMT research depends heavily on animal studies with mice being most often

Assay	Cell Lines Used	Similar Results with X-rays and Gamma Rays?
MTT (cytotoxicity)	HBEC-2, HBEC-13, HFL-1, A549, HeLa, MCF-7	Yes
Cell Migration	A549, HeLa	Yes
Colony Formation	A549	Yes
Western Blot	HBEC-2	Yes

Table 1.1. Record of successes in using X-rays from an X-RAD 320 Unit to achieve similar results as were obtained with a Cs-137 gamma-ray source, for specific cell culture assays widely used in radiobiological and other research.

used. During BMT with mice, the recipient mice may receive a genetically identical bone marrow graft (called a *syngeneic* graft), or a genetically different graft (called an *allogeneic* graft). If an allogeneic bone marrow graft (which is not matched at what is called the major histocompatibility complex, MHC) is transplanted, a severe immune system reaction can occur when the grafted cells attack the tissues of the individual receiving the bone marrow (graft-versus-host disease, GVHD). However, if the MHC antigens on the transplanted bone marrow cells match those of the host immune system, no GVHD is expected. A further complication can occur should the immune system of the host not be sufficiently suppressed (e.g., via high-dose irradiation) before allogeneic bone marrow transplantation. Should that be the case, rejection by the host's immune system of the grafted foreign bone marrow (host-versus-graft disease) can occur, particularly if an unmatched MHC exists. In addition, in cases of incomplete bone marrow ablation in the host, the host bone marrow can out-compete the donor bone marrow resulting in reconstitution of the hematopoietic system with immune cells of syngeneic origin, rather than donor allogeneic origin. Mouse models of BMT are routinely used to study GVHD, transplant rejection and whether aspects of the immune system depend on hematopoietic or somatic cells. Bone marrow transplantation studies at LRRI using mice focused on both allogeneic and syngeneic grafts. The allogeneic grafts were MHC-matched to avoid GVHD. The objective was to demonstrate that similar success in host bone marrow ablation and reconstitution with donor bone marrow can be obtained using X-rays from our X-RAD 320 Unit as is achieved with ^{137}Cs7 gamma rays from our Gammacell® 1000 Unit.

Two studies using mice (C.B-17 strain) and two irradiators (X-RAD 320 Unit and Gammacell® 1000 Unit) were conducted at LRRI and the study designs are briefly summarized below. For mouse studies with X-rays, a hardened photon energy spectrum (Filter #2, half value layer $\cong$ 3.7 mm Cu) was used to reduce the risk of skin damage associated with low-energy photons.

Study 1: Whole-body irradiation of C.B-17 mice with both irradiators and assessment of a) bone marrow and spleen cell depletion, b) body weight loss and recovery, and c) reconstitution of spleen and bone marrow cellularity after 6 weeks in the absence of a bone marrow transplant. Whole-body gamma-ray doses were 2.03 Gy (low), 4.01 Gy (moderate) and 6.0 Gy (high). Corresponding X-ray doses were 1.56 Gy (low), 3.09 Gy (moderate), and 4.62 Gy (high), based on our

central estimate of 1.3 for the RBE for killing (based on cytotoxicity studies at LRRI and literature search results).

Study 2: Whole-body irradiation of C.B-17 mice with both irradiators, followed one day later by delivery of bone marrow from either syngeneic (C.B-17) or allogeneic (B10.D2) donors and assessment of a) body weight loss and recovery and b) reconstitution of spleen and bone marrow cellularity 6 weeks after bone marrow transplantation. Flow cytometric evaluation of splenocytes was used to determine the extent of donor bone marrow engraftment. Gamma- and X-ray doses were the same as for Study 1.

Details related to the two mouse studies and dose-response relationships obtained are presented in the paper by Scott et al.[7] prepared for the Dose-Response Journal. Bone marrow was ablated to similar extents using high, moderate and low doses of X-rays and gamma rays. This supports our assumed X-ray RBE of 1.3 relative to gamma rays for killing of bone marrow cells. However, the number of viable splenocytes remaining 24 hours after low-dose gamma-ray exposure was significantly lower than the number following low-dose X-ray exposure, suggesting that the X-ray RBE for killing of splenocytes relative to gamma rays was <1.3. The lower X-ray RBE is also supported by the fact that splenocyte cell numbers six weeks after irradiation were significantly less in the mice exposed to the high dose of gamma rays compared to the high dose of X-rays.

Successful engraftment of allogeneic bone marrow was achieved only with gamma-ray doses of 4.01 and 6 Gy but not with any of the X-ray doses used. The lack of success of X-rays to allow engraftment of donor bone marrow was not expected and larger doses are likely needed to insure such engraftment. The need for larger doses likely relates to hematopoiesis that takes place in the remaining spleen tissue, leading to repopulation of the depleted bone marrow, apparently because of a lower X-ray RBE for killing of splenocytes than for killing of bone marrow cells.

Needed Follow-On Studies

New studies would have to be initiated to resolve whether bone marrow transplantation studies using C.B-17 mice can successfully be carried out using the X-RAD 320 Unit. Such studies would need to be supported by cell culture cytotoxicity studies that focus on bone marrow cells and splenocytes. The cytotoxicity studies conducted at LRRI focused on human bronchial epithelial cells, human lung fibroblast, and three types of human cancer cells so that none of the RBEs derived using Filter #2 may apply to bone marrow cells and splenocytes in mice. Research findings presented in Appendix A (published paper by Scott et al. 2012) indicated that RBE for cytotoxicity depends on the cell type irradiated and on the exposure geometry. The LRRI bone-marrow ablation and transplantation studies results suggest an X-Ray RBE <1.3 relative to ^{137}Cs gamma rays for killing of splenocytes in live mice. If so, X-ray doses would need to be larger than those used when Filter #2 is used on the X-RAD 320 Unit. The LRRI staff is quite willing to participate in any needed follow-on radiobiological research involving small animals and cells in culture that are exposed to X-rays from the X-RAD 320 or Gammacell® 1000 units.

Other Radiobiological Studies that Could Be Carried Out Using an X-RAD 320 Unit or a Cesium-137 Unit

Cell Culture Studies

- DNA damage/repair
- Genomic instability
- Bystander effects
- Adaptive response
- Mutagenesis
- Neoplastic transformation
- Epigenetic changes
- Co-culture
- Media-transfer
- Other

Studies with Mice or Rats

- Carcinogenesis
- Tissue reactions (deterministic effects)
- Adaptive response
- Acute lethality (hematopoietic, gastrointestinal, and CNS syndromes)
- Hematological effects
- Respiratory dysfunction
- Skin damage
- Fibrosis
- Cataracts
- Radiation-therapy-related (low- and high-dose therapy)
- Genetic susceptibility
- Other

Chapter 2

Issues Related to Replacing Cs-137 Sources with X-ray Units

In addition to the conclusions provided in the peer-reviewed publications (see Appendices A and B), there were additional observations related to the operation of the Gammacell® 1000 and the X-RAD 320. These observations are provided below. These are important considerations for any facility considering replacing a gamma-ray irradiator with an X-ray system such as the one used here.

Maintenance costs for X-ray units such as X-RAD 320 can be significantly higher than for a ^{137}Cs unit if annual service contracts are used as is being done at LRRI. Aging ^{137}Cs units may be an exception since breakdown may be rather frequent and replacement parts difficult to find as is now the case at LRRI.

Room temperature buildup can be a problem for X-ray units using an oil-to-air cooling system. Initially the room air conditioning system at LRRI was not adequate as room temperature buildup led to automatic shutdown of the X-RAD 320 unit. The air conditioning system had to be significantly improved at a cost to solve the temperature buildup problem.

Additional observations include the following:

- The aging Gammacell® 1000 Unit at LRRI broke down occasionally during this 2-year project. Repairs were very expensive and led to the unit being out of service for more than a week.
- The X-RAD 320 Unit's adjustable shelf for mounting samples or animals to be irradiated broke down the first time it was lowered. This led to the unit having to be repaired but at no extra cost.
- The X-RAD 320 Unit has so far only been used in one project while the Gammacell® 1000 Unit has been used in several projects and is therefore more heavily used. Thus, it is not known how well the X-RAD 320 Unit would hold up if used on a regular basis in multiple projects.
- For use of X-ray units in place of ^{137}Cs units in large transfusion medicine programs, throughput may be problematic and back-up plans may be necessary in case the X-ray unit needs to be taken out of service for breakdown-related repairs and for extended maintenance.

- Disposition of a ^{137}Cs irradiator will add to the cost of replacement with an X-ray unit, but recycling of the source may be possible through the U.S. Department of Energy's Off-Site Source Recovery Program.

Chapter 3

Deliverables

Two peer-reviewed publications were prepared by LRRI to document the feasibility of using x rays for the irradiation of biological specimens: one addressed the results of the work using cell cultures and one addressed the mouse studies. These publications were submitted to Radiation Protection Dosimetry and Dose-Response, which were critical in terms of establishing credibility for this work in the research community.

The peer-reviewed publications resulting from this effort are of interest to researchers performing radiobiological studies using ^{137}Cs, ^{60}Co, and machine generated x rays. These researchers are currently working in hospitals, universities, and government-funded and private research institutions throughout the U.S. and other countries. LRRI scientists that are engaged in radiobiological research are key contributors to the work described in this work.

The authors refer readers to the conclusions addressed in the following publications.

This page intentionally left blank.

References

[1] Radiation source use and replacement. Technical report, National Research Council of the National Academies, 2008.

[2] R. W. Borchardt. Strategy for the security and use of cesium-137 chloride sources. Policy Issue SECY-08-0184, 2008. U. S. Nuclear Regulatory Commission.

[3] L.W. Connell, S.W. Longley, R.K. Patel, and M. Wald-Hopkins. Cesium chloride irradiator replacement study: Replacement costs and alternative technologies. SAND Report (draft) 2013-XXXX, Sandia National Laboratories, 2013.

[4] Precision X-Ray, Inc., N. Branford, CT. *X-RAD 320 Users Manual*, 2010. Document Number: X-RAD320UM-UG.

[5] Atomic Energy of Canada Limited (AECL). *Gammacell 1000 Operator's Manual for Serial Numbers 37 and Up*, 3 edition, 1984. Technical Publications Document No. IN-J1100-83-04A.

[6] B. R. Scott, J. Hutt, Y. Lin, M. T. Padilla, K. M. Gott, and C. A. Potter. Biological microdosimetry based on radiation cytotoxicity data. *Radiation Protection Dosimetry*, 2012. Published on internet: doi:10.1093/rpd/ncs133, in press.

[7] B. R. Scott, K. M. Gott, C. A. Potter, and J. Wilder. A comparison of in vivo cellular responses to Cs-137 gamma rays and 320-kV X rays. *Dose Response*, 2013. Published on internet: doi:10.2203/dose-response.12-050.Scott, in press.

This page intentionally left blank.

Appendix A

Biological Microdosimetry Based on Radiation Cytotoxicity Data

The following pages contain the first deliverable provided by LRRI.

Radiation Protection Dosimetry Advance Access published August 5, 2012

Radiation Protection Dosimetry (2012), pp. 1–8 doi:10.1093/rpd/ncs133

BIOLOGICAL MICRODOSIMETRY BASED ON RADIATION CYTOTOXICITY DATA

B. R. Scott[1,*], J. Hutt[1], Y. Lin[1], M. T. Padilla[1], K. M. Gott[1] and C. A. Potter[2]
[1]Lovelace Respiratory Research Institute, Albuquerque, NM, USA
[2]Sandia National Laboratories, Organization 00545, Albuquerque, NM, USA

*Corresponding author. bscott@lrri.org

Received December 15 2011, revised June 27 2012, accepted July 11 2012

Researchers in the field of radiation microdosimetry have attempted to explain the relative biological effectiveness (RBE) of different ionising photon radiation sources on the basis of the singly stochastic, microdose metric lineal energy *y*, which only addresses physical stochasticity related to energy (ε) deposition via single events in the critical targets (cell nuclei assumed here). Biological stochasticity related to variable nuclei geometries and cell orientations (relative to the incoming radiation) is usually not addressed. Here a doubly stochastic microdose metric, the *single-event hit size q* ($=\varepsilon/T$), is introduced which allows the track length *T* to be stochastic. The new metric is used in a plausible model of metabolic-activity-based *in vitro* cytotoxicity of low-dose ionising photon radiation. The cytotoxicity model has parameters $E\{q\}$ (*average single-event hit size with q assumed to be exponentially distributed*) and $E\{\alpha\}$, which is the average value of the cellular response parameter α. $E\{\alpha\}$ is referred to as the *biological signature* and it is independent of *q*. Only $E\{q\}$ is needed for determination of RBE. The model is used to obtain *biological-microdosimetry-based q spectra* for 320-kV X-rays and ^{137}Cs gamma rays and the related RBE for cytotoxicity. The spectra are similar to published lineal energy *y* spectra for 200-kV X-rays and ^{60}Co gamma rays for 1-μm biological targets.

INTRODUCTION

Research conducted at Lovelace Respiratory Research Institute (LRRI) in conjunction with others at Sandia National Laboratories (SNL) focuses on comparing the relative biological effectiveness (RBE) of X-rays from an X-RAD 320 Unit[1] with gamma rays from a ^{137}CsCl irradiator (Gammacell 1000 Unit[2]). Such research facilitates evaluation of the feasibility of replacing existing ^{137}CsCl irradiators (a national security concern) with X-ray units such as X-RAD 320. Initially, the comparison was intended to rely fully on lineal energy *y* spectra differences for the two radiation sources to explain the RBE of 320-kV unit X-rays compared with ^{137}Cs gamma rays as has been done by others[3–5].

The singly stochastic microdose metric *y* as used here represents the radiation *hit size* (single-event) to the critical target (which can be sub-nuclear) and is formally defined as $y=\varepsilon/E\{l\}$, where ε (sometimes indicated as ε_1) is the energy impartation to the microscopic biological target in a single event (e.g. traversal of an ionisation-related electron)[6–9]. The variable *l* is a chord length through the critical target. The statistic $E\{\}$ represents the expectation value (i.e. average) of the quantity indicated (e.g. *l*, ε, etc.) between the brackets. For conducting physical measurements of *y* spectra, the target geometry is usually assumed fixed [e.g. tissue-equivalent microsphere (e.g. nucleus surrogate) with a fixed diameter] and measurements are carried out using a special spherical radiation detection device (e.g. Rossi counter).

After some study it was realised that with use of *y*, biological stochasticity related to the particle track length *T* varying over different paths within and through the biological targets of differing geometries (e.g. different sizes) has not been previously addressed for external ionising photon radiation. Here, the track length *T* refers to the incident particle (ionisation-produced electrons) track length within the biological target plus the track lengths within the target of all secondary electrons.

In this paper, a novel microdose metric is introduced that allows addressing both physical and biological stochasticity influences on the distribution of photon radiation single-event hit sizes to the critical microscopic targets of irradiated cells in culture. The metric is the *doubly stochastic, single-event, hit size* $q=\varepsilon/T$. It is also shown how *q* spectra can be generated on the basis of *biological microdosimetry* (concept introduced some years ago by Scott and Schöllnberger[10]) when a plausible formal distribution is assigned to *q*. While cell nuclei have been assumed by others to be the critical targets, the methodology used and results obtained apply irrespective of the size distribution of the critical microscopic targets.

METHODS

Cell culture preparations and irradiations

This radiation cytotoxicity study involves use of cultures of normal human bronchial epithelial cells (HBEC-13 and HBEC-2) with oval-shaped nuclei

© The Author 2012. Published by Oxford University Press. All rights reserved. For Permissions, please email: journals.permissions@oup.com

(Figure 1 for HBEC-13). In preparing for cytotoxicity studies, HBEC-13 and HBEC-2 cells (passage number <10) were cultured on fibronectin (Athenaes)-coated plates, in keratinocyte serum-free medium, supplemented with bovine pituitary extract and rEGF (Invitrogen). Cells were cultured at 37°C, 5 % CO_2. They were plated at $\sim 5 \times 10^4$ cells per 35-mm dish and were incubated overnight and irradiated on the next day. The cells were dispersed as randomly oriented (in two-dimensions) single cells in culture (i.e. without clumping) (Figure 1 for HBEC-13).

Cytotoxicity evaluations

Cytotoxicity due to X-rays and that due to gamma-rays to cultured cells were assessed using the MTT [3-(4,5-dimethylthiazol-2-yl)-2,5-diphenyltetrazolium bromide, *a yellow tetrazole*] colorimetric assay. As cytotoxicity increases as a result of radiation exposure, the level of reduction (relative to controls) of injected MTT (yellow colour) to formazan dyes (*purple colour*) decreases. The decrease in metabolic activity is likely a continuous function of the radiation energy deposited in the critical target and is used as a measure of cytotoxicity. Only MTT assay recordings below the minimum for controls were considered a radiation-induced cytotoxic event. Six samples were used for each dose group (control, low, medium and high). The cytotoxic events (i.e. exceeding the MTT assay threshold) over different samples were assumed to have a *binomial distribution*, with the associated probability $P(D)$ of cytotoxicity evaluated as discussed in the following section. Cytotoxicity was evaluated at 48 h after radiation exposure. The data generated are presented in Table 1.

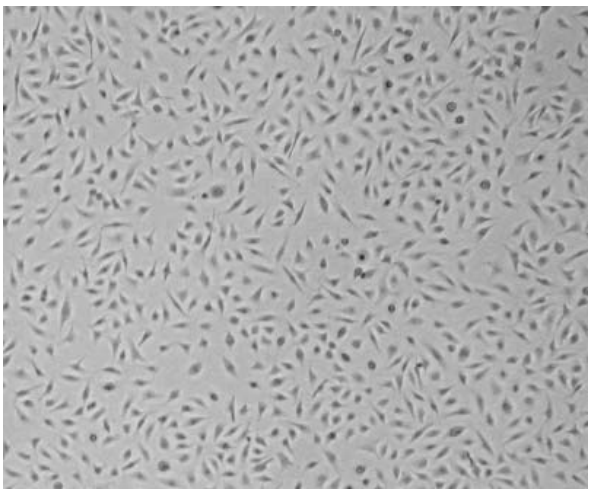

Figure 1. Randomly oriented human bronchial epithelial (HBEC-13) cells in culture.

Radiation sources

Two radiation sources were used: (1) Gammacell 1000 Unit[2] with a horizontal beam and (2) X-RAD 320 Unit[1] with a vertical beam. Gamma-ray doses were evaluated on the basis of nanoDOT™ (Landauer, Inc.) measurements within empty exposure dishes. The nanoDOTs were calibrated for ^{137}Cs gamma rays. Minimum shielding was used for the gamma-ray exposures. X-ray doses were based on X-RAD 320 Unit calibrations for the source to target distance (50 cm) and a 2.0-mm aluminium filter (half value layer ≅ 1.0 mm Cu), and no focusing. All doses were delivered within seconds so that dose-rate-effect-related differences between X-ray and gamma-ray exposures were not expected.

Table 1. MTT-assay-based cytotoxicity data for gamma- and X-ray exposure of HBEC-13 and HBEC-2 cells in culture.

Cell type	Radiation type	Dose (mGy)	Number of MTT samples	Cytotoxicity threshold exceedances	Exceedances standard error[a]
HBEC-13	None	0	6	0	
HBEC-13	Gamma rays	470	6	0	<0.9
HBEC-13	Gamma rays	940	6	1	0.9
HBEC-13	Gamma rays	1880	6	3	1.2
HBEC-13	X-rays	360	6	0	<0.9
HBEC-13	X-rays	720	6	0	<0.9
HBEC-13	X-rays	1440	6	4	1.2
HBEC-2	Gamma rays	470	6	0	<0.9
HBEC-2	Gamma rays	940	6	5	0.9
HBEC-2	Gamma rays	1880	6	3	1.2
HBEC-2	X-rays	360	6	3	1.2
HBEC-2	X-rays	720	6	3	1.2
HBEC-2	X-rays	1440	6	6	<0.9

[a]Based on an assumed binomial distribution of cytotoxicity threshold exceedances.

RESULTS

Biological microdosimetry approach to *q* spectra generation and RBE evaluation for the low-dose region

The focus here is on cell killing *in vitro* by *low doses* of ionising photon radiation. It is assumed that radiation-induced cell killing (cytotoxicity) arises as a *Poisson process* with expectation value $k\{q \text{ spec}, \alpha \text{ spec}\}D$ for killed cells among N irradiated, where D is the radiation absorbed dose and $k\{q \text{ spec}, \alpha \text{ spec}\}$ is a parameter that depends on the q spectrum (q spec) and also on the spectrum (α spec) for the *cellular response parameter* α, which reflects the varying biological characteristics of the target cells. It follows that the cytotoxicity probability $P(D)$ after low doses is given by the following:

$$P(D) = 1 - \exp(-k\{q \text{ spec}, \alpha \text{ spec}\}D) \tag{1}$$

Because $k\{q \text{ spec}, \alpha \text{ spec}\}$ depends on the q spectrum, it also depends on the energy characteristics of the photon radiation source, the exposure geometry (impacted by shielding and filters) and orientations of the target cells relative to the incoming ionising photon radiation beam. Because cell culture samples are not exactly identical biologically, the parameter α varies over different samples and hence the need for addressing the α spectrum (i.e. probability density).

For the cell culture studies of this research, target cells are randomly oriented in two-dimensions (Figure 1 for HBEC-13) for both HBEC-13 and HBEC-2 cells when observed under a microscope. The q spectrum is expected to be influenced by the cell orientation distribution and radiation exposure geometry (which differs for the gamma- and X-ray sources used in this study). $k\{q \text{ spec}, \alpha \text{ spec}\}$ was evaluated as a weighted sum over the q and α spectra:

$$k\{q \text{ spec}, \alpha \text{ spec}\} = \int_a^b \int_0^\infty k\{q, \alpha\} f(\alpha) f(q) \mathrm{d}\alpha \, \mathrm{d}q \tag{2}$$

For the application of Equation (2) to biological data, a is the minimum value for α and b is the maximum. The stochastic variable q with the unit keV μm^{-1} is assigned a minimum value of 0 keV μm^{-1} and a maximum value of ∞ (keV μm^{-1}). The functions $f(\alpha)$ and $f(q)$ are the probability densities of α and q, respectively, and $f(q)$ is evaluated on the basis of biological microdosimetry. Since only low-LET photon sources and low-absorbed radiation doses are considered here, the following plausible form is assigned to the *hit size effectiveness function* $k\{q, \alpha\}$:

$$k\{q, \alpha\} = \alpha q \tag{3}$$

Thus, the hit size effectiveness is proportional to q. The hit size effective function $k\{q, \alpha\}$ when multiplied by the absorbed dose D gives the expected number of lethal events per target cell when each single-event energy deposition in the critical biological target has hit size q. The notion of such a hit size effectiveness function was introduced years ago for microdosimetric modelling of radiation biological effects[11, 12]. Equation (3) implicates the parameter $k\{q \text{ spec}, \alpha \text{ spec}\}$ as increasing as the mean radiation hit size $E\{q\}$ increases for ionising photon radiation. Implied is that wasting of radiation dose is negligible when the absorbed radiation dose D is low. It follows from Equations (2) and (3), irrespective of the mathematical forms for $f(q)$ and $f(\alpha)$, that $k\{q \text{ spec}, \alpha \text{ spec}\}$ is given by:

$$k\{q \text{ spec}, \alpha \text{ spec}\} = E\{\alpha\}E\{q\} \tag{4}$$

$E\{\alpha\}$ (a deterministic quantity) is the expectation value for the cellular response parameter α and is called the *biological signature.* $E\{q\}$ (a deterministic quantity) represents the *expected single-event hit size.* The biological signature $E\{\alpha\}$ does not depend on the q spectrum. $E\{q\}$ clearly depends on the q spectrum which is influenced by target cell geometries and orientations relative to the incident radiation beam as already indicated. With biological microdosimetry, the study was focussed on obtaining estimates of $E\{\alpha\}$, $E\{q\}$ and $k\{q \text{ spec}, \alpha \text{ spec}\}$ and functions (e.g. RBE) of these endpoints based on fitting the cytotoxicity model to actual data (based on cell metabolic status). This can be achieved using Bayesian inference implemented using Markov chain Monte Carlo, as is done here.

Using Equation (4), the low-dose RBE for ionising photon radiation with q-spectrum 1 relative to ionising photon radiation with q-spectrum 2 is evaluated as follows:

$$\text{RBE}\{1, 2\} = \frac{E\{q_1\}}{E\{q_2\}} \tag{5}$$

The X-ray RBE for the X-RAD 320 Unit relative to ^{137}Cs gamma rays has been evaluated for cytotoxicity to HBEC-13 and HBEC-2 cells in culture. The two cell lines were derived from different individuals and were established with the same method but may have quite different *genetic characteristics and epigenetic statuses* since sensitivity to neoplastic transformation by cigarette smoke carcinogens differs for the two cell lines (unpublished observation).

For the gamma-ray exposure, minimal shielding was used and the incident beam was horizontal and the target cell dishes were rotated during irradiation. For the X-ray exposure, the target dishes were stationary with the X-ray beam coming from above the target cells. Thus, *the RBE estimates obtained are specific to the exposure geometries.* No radiation transport calculations are needed to obtain q spectra, since their derivations are based on biological microdosimetry.

The cytotoxicity probability was evaluated on the basis of data obtained using the MTT assay as previously indicated. Gamma-ray absorbed doses were ~470, 940 and 1880 mGy. X-ray absorbed doses were ~360, 720 and 1440 mGy. Unirradiated controls were also used.

Equations (1) and (4) were applied to the cytotoxicity data assuming a binomial distribution of cytotoxic events over each of six different samples at each of three dose levels. Markov chain Monte Carlo evaluations were carried out using the WinBUGS software[13]. Broad, uniform prior distributions were used for all free parameters with the bound on $E\{q_\gamma\}$ for gamma rays set based on published y spectra[5, 12] for gamma-ray-exposed mammalian cells in culture. The lower and upper bounds for the prior distribution for $E\{q_\gamma\}$ were 0.1 and 50 keV μm^{-1}, respectively. $E\{q_x\}$ for X-rays was evaluated as the product RBE$\times E\{q_\gamma\}$, with RBE evaluated as a free parameter, with lower and upper bounds of 1 and 2, respectively. The bounds are based on low-dose RBEs for cytotoxicity reported by Nikhoo and Linborg[14].

The X-ray and gamma-ray cytotoxicity data for HBEC-13 and HBEC-2 cells were first fitted simultaneously to obtain a best estimate of the biological signature $E\{\alpha\}$ (evaluated on the basis of the posterior distribution mean) and its related uncertainty (evaluated on the basis of specific percentiles of the posterior distribution). The posterior distribution mean of $E\{\alpha\}$ was then used as a fixed value in a second run where again the combined X-ray and gamma-ray data were used. The second run allowed simultaneous evaluation of $E\{q_\gamma\}$, $E\{q_x\}$, RBE, $k\{q$ spec$_x$, α spec$\}$ for X-rays and $k\{q$ spec$_\gamma$, α spec$\}$ for gamma rays based on posterior distribution means and conditional on the estimate of $E\{\alpha\}$. Percentiles of the posterior distributions for these parameters provided measures of uncertainty, also conditional on the estimate used for $E\{\alpha\}$ in this study. The prior distribution used of $E\{\alpha\}$ was uniformly distributed from 10^{-5} to 10^{-3} μm keV^{-1} mGy^{-1}.

Estimates (posterior distribution means and standard deviations) obtained for key model parameters (and the RBE) for X- and gamma-ray exposure of HBEC-13 cells were as follows: mean$\{E\{\alpha\}\}=2.1(\pm 2.5)\times 10^{-4}$ μm keV^{-1} mGy^{-1}, mean$\{E\{q_\gamma\}\}=1.3(\pm 0.4)$ keV μm^{-1}, mean$\{E\{q_x\}\}=1.8(\pm 0.6)$ keV μm^{-1}, mean$\{k\{q$ spec$_\gamma$, α spec$\}\}=2.7(\pm 0.95)\times 10^{-4}$ mGy^{-1}, mean$\{k\{q$ spec$_x$, α spec$\}\}=3.9(\pm 1.4)\times 10^{-4}$ mGy^{-1} and mean$\{$RBE$\}=1.5$ for X-rays relative to gamma rays. Lower and upper bounds of 1 and 2 were imposed for the RBE for reasons previously indicated. The notation mean$\{\}$ refers to the posterior distribution mean of the indicated quantity. Posterior distribution percentiles related to these parameters (except for $E\{\alpha\}$ and RBE) are presented in Table 2. The posterior distribution for $E\{\alpha\}$ appeared to be exponential. The 2.5, 5, 25, 50, 75, 95 and 97.5 % percentiles expressed in μm keV^{-1} mGy^{-1} were respectively (0.11, 0.13, 0.32, 0.99, 3.1, 7.9 and 8.9)$\times 10^{-4}$.

Estimates (posterior distribution means and standard deviations) obtained for key model parameters (and RBE) for X- and gamma-ray exposure of HBEC-2 cells were as follows: mean$\{E\{\alpha\}\}=2.0(\pm 2.3)\times 10^{-4}$ μm keV^{-1} mGy^{-1}, mean$\{E\{q_\gamma\}\}=4(\pm 1)$ keV μm^{-1}, mean$\{E\{q_x\}\}=6.5(\pm 1.6)$ keV μm^{-1}, mean$\{k\{q$ spec$_\gamma$, α spec$\}\}=8.2(\pm 2.0)\times 10^{-4}$ mGy^{-1}, mean$\{k\{q$ spec$_x$, α spec$\}\}=1.3(\pm 0.33)\times 10^{-3}$ mGy^{-1}and mean$\{$RBE$\}=$ 1.6 for X-rays relative to gamma rays. Lower and upper bounds of 1 and 2 were imposed for the RBE for reasons previously indicated. Posterior distribution percentiles related to these parameters (except for $E\{\alpha\}$ and RBE) are presented in Table 3. The posterior distribution for $E\{\alpha\}$ appeared to be exponential. The 2.5, 5, 25, 50, 75, 95 and 97.5 % percentiles in units of μm keV^{-1} mGy^{-1} were respectively (0.15, 0.18, 0.4, 1.0, 2.8, 7.5 and 8.6)$\times 10^{-4}$.

The variability indicated in Tables 2 and 3 may in part reflect the variability in the MTT assay results

Table 2. Posterior distribution statistics for parameters and variables for X-ray and gamma-ray cytotoxicity to HBEC-13 cells in culture[a].

Parameter or variable	Percentile of posterior distribution						
	2.5 %	5 %	25 %	50 %	75 %	95 %	97.5 %
$E\{q_\gamma\}$ (keV μm^{-1})	0.559	0.642	0.952	1.22	1.54	2.08	2.29
$E\{q_x\}$ (keV μm^{-1})	0.802	0.924	1.37	1.75	2.2	3.0	3.31
$k\{q$ spec$_\gamma$, α spec$\}$	1.19E−4	1.37E−4	2.03E−4	2.60E−4	3.28E−4	4.43E−4	4.87E−4
$k\{q$ spec$_x$, α spec$\}$	1.71E−4	1.97E−4	2.91E−4	3.73E−4	4.68E−4	6.38E−4	7.05E−4

[a]Results obtained with the biological signature $E\{\alpha\}$ fixed at 2.1×10^{-4} μm keV^{-1} mGy^{-1}.

Table 3. Posterior distribution statistics for parameters and variables for X-ray and gamma-ray cytotoxicity to HBEC-2 cells in culture[a].

Parameter or variable	Percentile of posterior distribution						
	2.5 %	5 %	25 %	50 %	75 %	95 %	97.5 %
$E\{q_\gamma\}$ (keV μm^{-1})	2.38	2.58	3.33	3.94	4.64	5.82	6.25
$E\{q_x\}$ (keV μm^{-1})	3.73	4.06	5.30	6.32	7.47	9.4	10.1
$k\{q$ spec$_\gamma$, α spec$\}$	4.8E−4	5.22E−4	6.72E−4	7.96 E−4	9.37E−4	1.18E−3	1.26E−3
$k\{q$ spec$_x$, α spec$\}$	7.54E−4	8.19E−4	1.07E−3	1.28E−3	1.51E−3	1.9E−3	2.04E−3

[a]Results obtained with biological signature $E\{\alpha\}$ fixed at 2.0×10^{-4} μm keV^{-1} mGy^{-1}.

and the small number of samples used. Thus, other less variable cytotoxicity assays or biomarker (of radiation absorbed dose) endpoints may prove even more reliable for biological microdosimetry for low-level radiation exposure.

Posterior distribution mean values of $E\{q_x\}$ and $E\{q_\gamma\}$ for X- and gamma-ray exposure of HBEC-2 and HBEC-13 cells have been used in generating distributions $qf(q)$. It was assumed that $f(q)$ could be adequately represented by one among the family of 2-parameter Weibull distribution functions. Distributions $qf(q)$ and qd(q) ($=q^2f(q)/E\{q\}$) based on the assigned value for $E\{q\}$ but having different shape parameters were generated and the spectra obtained with published results for $yf(y)$ and $yd(y)$ ($=y^2f\{y\}/E\{y\}$) were visually compared and it was found that only values for a shape parameter of 1 (implicating an exponential distribution of q) yielded spectra that were similar to published y spectra ($yf(y)$ or $yd(y)$). An exponential distribution, λ exp($-\lambda$ q), with parameter λ, of the single-event hit sizes q was therefore assumed with $\lambda_x=1/\text{mean}\{E\{q_x\}\}$ for X-rays and $\lambda_\gamma=1/\text{mean}\{E\{q_\gamma\}\}$ for gamma rays. Many hit sizes associated with the indicated exponential distributions will exceed mean$\{E\{q_x\}\}$ and mean$\{E\{q_\gamma\}\}$, and thus, use of an exponential distribution does not necessarily limit the single-event hit sizes to be small.

The X-ray and gamma-ray spectra obtained for $qf(q)$ for HBEC-13 cells are presented in Figure 2. Corresponding results for HBEC-2 cells are presented in Figure 3. It is emphasised that the *q spectra are solely based on biological microdosimetry* but are similar to what was reported for 1-μm size targets (sub-nuclear) by Okamoto *et al.*[1] for y spectra for 200-kV X-ray and ^{60}Co gamma-ray exposure of human salivary gland tumour cells. Their spectra were derived using a tissue-equivalent proportional counter and using theoretical Monte Carlo simulation (radiation transport calculations). A similar y spectrum for 200-kVp X-rays was also reported by Varma *et al.* [12] for 1 μ biological targets based on radiation transport calculations.

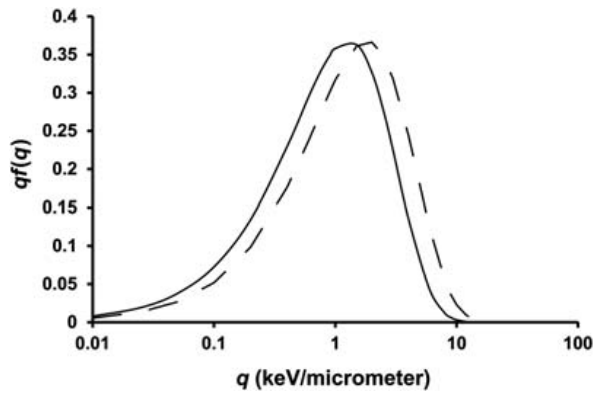

Figure 2. Biological-microdosimetry-based dose distributions $q_\gamma f(q_\gamma)$ (smooth curve) and $q_x f(q_x)$ (dashed curve) in HBEC-13 cell nuclei for the single-event hit size q for ^{137}Cs gamma rays and 320-kV X-rays.

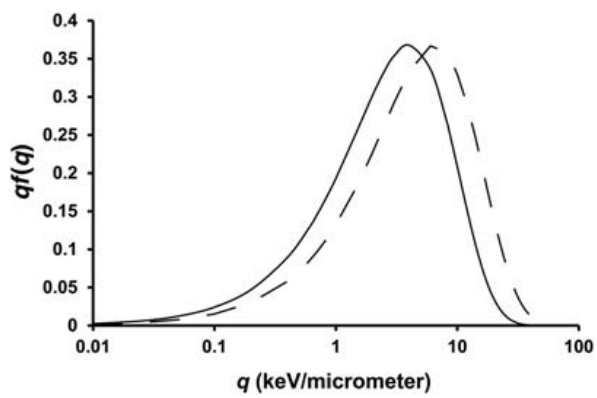

Figure 3. Biological-microdosimetry-based dose distributions $q_\gamma f(q_\gamma)$ (smooth curve) and $q_x f(q_x)$ (dashed curve) in HBEC-2 cell nuclei for the single-event hit size q for ^{137}Cs gamma rays 320-kV X-rays.

The results presented in Figures 2 and 3 are based on assigned fixed values of $E\{\alpha\}$ for the two cell lines that were derived using uniform prior distributions. Analysis for HBEC-2 cells was conducted where instead of using a uniform prior distribution

for $E\{\alpha\}$, a very different exponential distribution with parameter $\lambda=1.38\times10^{4}$ μm^{-1} keV mGy was used . The mode of the distribution is at zero and the mean is $1/\lambda=7.25\times10^{-5}$ μm keV^{-1} mGy^{-1}. The distribution gives very low probability to values of $\alpha > 0.001$ μm keV^{-1} mGy^{-1}, which is the upper bound for the uniform distribution that was used. The posterior distribution mean obtained for $E\{\alpha\}$ was 1.5 times smaller than the value obtained with the uniform prior distribution. Decreasing the value of $E\{\alpha\}$ by a factor K would correspondingly increase $E\{q\}$ by the same factor because of the constraint imposed by Equation (4). Similarly, increasing $E\{\alpha\}$ by a factor of K would correspondingly reduce $E\{q\}$ by the same factor. Thus, results obtained in this paper can be adjusted for any desired value of $E\{\alpha\}$.

In addition to using a fixed value for $E\{\alpha\}$, a uniform prior distribution was also assigned to $E\{q\}$ to obtain the results presented in Figures 2 and 3. Therefore, an analysis was conducted to see the impact of assigning a very different prior distribution to $E\{q\}$. In this case, an exponential distribution was also assigned but with parameter $\lambda = 0.276$ μm keV^{-1}, which has a mode at zero and a mean of 3.62 keV μm^{-1}, and assigns very little probability to values of $q > 50$ keV μm^{-1} (upper bound used for uniform distribution). For HBEC-2 cells, the posterior distribution means of $E\{q_\gamma\}$ and $E\{q_x\}$ changed (decreased) by 5 and 6 %, respectively, implicating a modest impact of the prior distribution assignment on these quantities. The corresponding decreases for HBEC-13 cells were 6 and 4 %, respectively. The posterior distribution means for the RBE were essentially the same (<2 % change) for the two prior distributions for $E\{q\}$, for both cell lines.

Assuming cytotoxicity to result from lethal nuclear DNA double-strand breaks (DSB), the expected Poisson distributions of lethal breaks per cell were calculated for both HBEC-13 and HBEC-2 cells exposed to 200, 400 or 800 mGy of 350-kV X-rays from the authors' X-RAD 320 Unit. The expected number of lethal breaks per cell is given by the product $k\{q \text{ spec}, \alpha \text{ spec}\}D$, with the slope parameter evaluated on the basis of the posterior distribution mean. The expected distributions of DSBs are presented in Figures 4 and 5 and suggest that the HBEC-2 cells may have a DNA DSB repair deficiency compared with the HBEC-13 cells because of the implicated larger number of observable breaks for HBEC-2 cells.

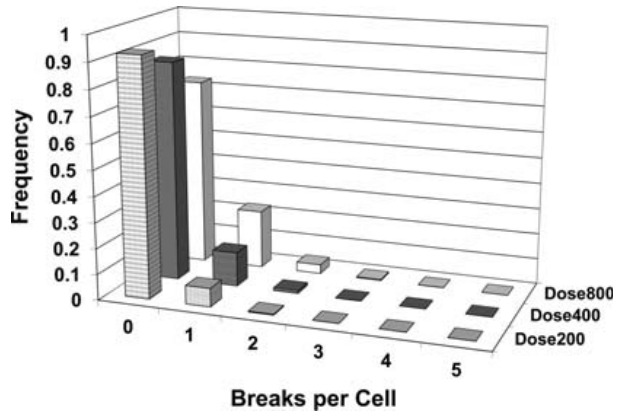

Figure 4. Expected distribution (Poisson) of lethal nuclear DNA double-strand breaks per cell after exposure of HBEC-13 cells in culture to absorbed doses of 200, 400 or 800 mGy of 350-kV X-rays from our X-RAD 320 Unit. The mean number of breaks per cell was evaluated as $3.89\times10^{-4}D$, for D in mGy.

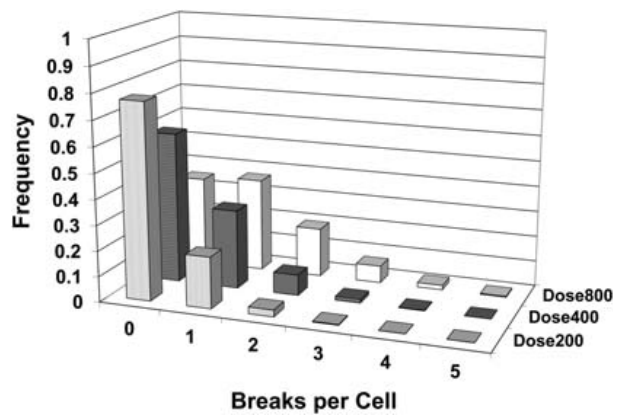

Figure 5. Expected distribution (Poisson) of lethal nuclear DNA double-strand breaks per cell after exposure of HBEC-2 cells in culture to absorbed doses of 200, 400 or 800 mGy of 350-kV X-rays from our X-RAD 320 Unit. The mean number of breaks per cell was evaluated as $1.31\times10^{-3}D$, for D in mGy.

DISCUSSION

Currently in the field of radiation microdosimetry, y spectra play an important role in explaining the RBE of X-rays relative to gamma rays[5]. This singly stochastic microdose metric can be calculated or measured using special counters such as Rossi tissue-equivalent proportional counters. Rossi counters are spherical chambers with *tissue-equivalent walls* and *tissue-equivalent gas* that fills the chamber. Their purpose is to simulate the stochastic radiation dose to small volumes of tissue such as the size of the cell nucleus when spherical.

The spherical shape of the chamber was chosen so that its response would be more or less independent of the direction from which radiation comes. These counters have been used for years in radiation microdosimetry. Here, the focus is on X- and gamma-ray microdosimetry. These photon radiation sources interact with the tissue-equivalent walls of the chamber and dislodge electrons (e.g. Compton

electrons) from atoms that traverse the tissue-equivalent gas that fills the chamber. The size of the pulse from the traversal reflects the ionisations produced in the gas by an electron along its track across the chamber. Because the detector chamber has a fixed, known geometry, the average chord length for particles traversing the chamber can be calculated. This allows measurement of y spectra for a given radiation source. Adjusting the pressure in the gas chamber allows simulation of y spectra for microscopic spherical volumes.

A key finding of the present study is that like physical stochasticity related to single-event energy deposition size for electrons from ionisation events, biological stochasticity is also likely to be important for explaining radiation cytotoxicity and RBE. We provide evidence (q-spectra-related) for RBE depending on the type of cells irradiated.

The posterior distribution means of $E\{q_\gamma\}$ for HBEC-13 and HBEC-2 cell lines were 1.3 and 4 keV μm^{-1}, respectively. These values can be compared with the very conservative upper bound of 50 keV μm^{-1} that was used for the uniform prior distribution that was assigned for $E\{q_\gamma\}$. The much lower values for the obtained posterior distribution means compared with the 50 keV μm^{-1} value indicate that it *is highly unlikely that average single-event gamma-ray hit sizes are much larger than a few keV μm^{-1} for the radiation sources used* in agreement with y spectra for nuclear- and sub-nuclear-sized targets. Assuming a systematic error factor of 1.5 (based on information already provided) related to the choice of the prior distribution for $E\{\alpha\}$ and a systematic error factor of 1.06 (based on information already provided) for the choice of prior distribution for $E\{q_\gamma\}$, the overall systematic error factor would be $1.5\times1.06=1.59$, which indicates that the posterior distribution mean of $E\{q_\gamma\}$ could be presumed to differ from the correct posterior distribution mean by not more than about a factor of 2.0.

The radiosensitivity of HBEC-2 cells relative to that of HBEC-13 cells was evaluated on the basis of the posterior distribution means of $k\{q\ \text{spec}_x,\ \alpha\ \text{spec}\}$ and $k\{q\ \text{spec}_\gamma,\ \alpha\ \text{spec}\}$. For gamma rays, the relative sensitivity$=8.2\times10^{-4}$ mGy^{-1}/2.7×10^{-4} mGy^{-1}=3.0. For X-rays, the relative sensitivity$=1.3\times10^{-3}$ mGy^{-1}/3.9×10^{-4} mGy^{-1}=3.3. Thus, *relative sensitivity appears to differ for both X-ray and gamma-ray sources* by a factor of about 3. For comparison, the relative sensitivity that would be expected if both radiation sources had the same q spectrum would be given by the ratio of the posterior distribution values of mean$\{E\{\alpha\}\}$, i.e. $2.0\times10^{-4}/2.1\times10^{-4}\cong1.0$ (units of $E\{\alpha\}$ omitted here). Assuming that DNA damage repair capacity influences the biological signature $E\{\alpha\}$ only, the indicated result implicates biological stochasticity influences on $f(q)$ for the two cell types as having an important role in determining their differential response to irradiation. *We hypothesise that $E\{\alpha\}$ will be positively correlated with genetic susceptibility status and negatively correlated with DNA repair capacity. We hope to conduct future studies to test these hypotheses.*

After this paper was originally submitted, additional MTT cytotoxicity data were acquired for three more cell lines (human cancer cells): A549, HeLa and MCF-7. The same three gamma-ray doses were used along with a control group; however, for the X-ray exposures a different filter comprised of 0.75-mm tin+0.25-mm copper+1.5-mm aluminium (half value layer $\cong$ 3.7-mm Cu) was used to harden the photon energy spectrum. The hardened energy spectrum was expected to reduce the X-ray RBE. X-ray doses for the low, moderate and high-dose groups were ~720, 1440 and 2890 mGy, respectively. Prior distributions for parameters were the same as used for HBEC-2 and HBEC-13 cells except that the upper bound for the uniform prior distribution of $E\{q\}$ was set at 40 instead of 50 keV μm^{-1} to speed up the Monte Carlo chain convergence, since the posterior mean$\{E\{q\}\}$ was <10 keV μm^{-1} for HBEC-2 and HBEC-13 cells for both X- and gamma-ray exposure.

The posterior distribution means and standard deviations of $E\{\alpha\}$ were as follows: A549 cells, mean$\{E\{\alpha\}\}=2.3(\pm2.5)\times10^{-4}$ μm keV^{-1} mGy^{-1}; HeLa cells, mean$\{E\{\alpha\}\}=2.6(2.5)\times10^{-4}$ μm keV^{-1} mGy^{-1}; MCF-7 cells, mean$\{E\{\alpha\}\}=2.3(\pm2.6)\times10^{-4}$ μm keV^{-1} mGy^{-1}. The large posterior distribution standard deviations obtained relate to the distributions appearing to be exponential.

Corresponding values of $E\{q_\gamma\}$ were as follows: A549 cells, 3.2 ± 0.7 keV μm^{-1}; HeLa cells, 3.8 ± 0.8 keV μm^{-1}; MCF-7 cells, 2.5 ± 0.5 keV μm^{-1}. Corresponding values of $E\{q_x\}$ were as follows: A549 cells, 4.6 ± 1.0 keV μm^{-1}; HeLa cells 4.5 ± 0.8 keV μm^{-1}; MCF-7 cells, 3.5 ± 0.7 keV μm^{-1}.

Corresponding values of the X-ray RBE evaluated as mean $\{E\{q_x\}/E\{q_\gamma\}\}$ were as follows: A549 cells, 1.5 ± 0.3; HeLa cells, 1.2 ± 0.2; MCF-7 cells, 1.4 ± 0.3. Microdosimetric spectra for q_γ and q_x can be generated on the basis of respective exponential distributions with parameters $\lambda_\gamma=1/\text{mean}\{E\{q_\gamma\}\}$ and $\lambda_x=1/\text{mean}\{E\{q_x\}\}$. The results obtained are consistent with a slight reduction in RBE because of hardening of the X-ray photon energy spectrum.

The q spectra generated apply irrespective of the size distribution and shapes of the critical biological targets and were achieved with far fewer resources than are needed for physical measurements or theoretical calculations involving radiation transport (computer-code related). However, the spectra produced may be modestly influenced by the prior distribution assigned for $E\{\alpha\}$ and to a lesser extent by the prior distribution for $E\{q\}$. The posterior distribution mean of RBE appears not to be sensitive to

the choice of the prior distributions. Given the findings presented in this paper, biological microdosimetry methods may eventually become widely used in the fields of microdosimetry and nanodosimetry as they relate to low-dose radiation biological effects.

Our findings indicate that X-ray sources such as the X-RAD 320 Unit can be used as successfully in studies of radiation cytotoxicity in culture as in the case of ^{137}Cs sources. However, a number of problems with the X-RAD 320 Unit, which has an oil-based cooling system, were experienced. A major problem was room temperature build-up causing automatic shutdown of the unit. Modification of the room air-conditioning system to provide for cooler air solved the temperature build-up problem.

CONCLUSONS

Biological stochasticity is expected to have a significant impact on the radiation single-event hit size distribution to critical microscopic biological targets and can be accounted for along with physical stochasticity using the novel microdose metric q.

The q spectra generated are similar to published spectra for 1-μm size (i.e. sub-nuclear) critical targets. Because of biological stochasticity, X-ray RBE relative to gamma rays is expected to depend on the types of cells exposed in addition to differences in exposure geometry. Biological microdosimetry aimed at generating q spectra can be employed at a relatively low cost compared with that for physical-measurement-based and radiation-transport-code-based microdosimetry for y spectra.

ACKNOWLEDGEMENTS

The authors express their thanks and appreciation to the U. S. Department of Energy, NA-22, Radiation Source Replacement Program and Frances Keel (DOE/NA-221). The authors are also grateful to Susan Longley of Sandia National Laboratories, whose vision and research related to use of ^{137}CsCl-gamma and X-ray irradiators in biological studies helped to pave the way for obtaining the novel results presented in this paper, and to the journal referees and Consultant Editor for their very helpful comments.

FUNDING

This work was performed under project number SL11-RadBio-PD13 and with partial support from the Office of Science (BER), U.S. Department of Energy, grant no. DE-FG02-09ER64783.

REFERENCES

1. Precision X-Ray, Inc. (PXINC). *X-RAD 320 Users Manual. Document Number: X-RAD320UM-UG.* Precision X-Ray, Inc. (2010).
2. Atomic Energy of Canada Limited (AECL). *Gammacell 1000 operator's manual for serial numbers 37 and up, Edition 3*. Technical Publications Document No. IN-J1100-83-04A. Atomic Energy of Canada Limited (1984).
3. International Commission on Radiation Units and Measurements ICRU). *Prescribing, recording, and reporting proton-beam therapy.* ICRU Report 78. Oxford University Press (2007).
4. Liu, C. S., Tung, C. J., Hu, Y. H., Chou, C. M., Chao, T. C. and Lee, C. C. *Calculations of specific cellular doses for low-energy electrons.* Nucl. Instrum. Methods B **267**, 1823–1829 (2009).
5. Okamoto, H., Kanai, T., Kase, Y., Matsumoto, Y., Furusawa, Y., Fujita, Y., Saitoh, H., Itami, J. and Kohno, T. *Relationship between lineal energy distribution and relative biological effectiveness for photon beams according to the microdosimetric kinetic model.* J. Radiat. Res. **52**, 75–81 (2011).
6. Kellerer, A. M. and Rossi, H. H. *The theory of dual radiation action*. Curr. Top. Radiat. Res. **8**, 85–158 (1970).
7. Kellerer, A. M. and Chmelevsky, D. *Concepts of microdosimetry. I. Quantities.* Radiat. Environ. Biophys. **12**, 61–69 (1975).
8. Kellerer, A. M. and Chmelevsky, D. *Concepts of microdosimetry. II. Probability distributions of the microdosimetric variables.* Radiat. Environ. Biophys. **12**, 205–216 (1975).
9. Kellerer, A. M. and Chmelevsky, D. *Concepts of microdosimetry. III. Mean values of the microdosimetric distributions.* Radiat. Environ. Biophys. **12**, 321–335 (1975).
10. Scott, B. R. and Schöllnberger, H. *Introducing biological microdosimetry for ionising radiation*. Radiat. Prot. Dosim. **91**(4), 377–384 (2000).
11. Varma, M. N., Bond, B. P. and Matthews, G. *Hit-size effectiveness theory applied to high doses of low-LET radiation for pink mutations in Tradescantia*. Radiat. Prot. Dosim. **13**(1–4), 307–309 (1985).
12. Varma, M. N., Wu, C. S. and Zaider, M. *Hit size effectiveness in relation to the microdosimetric site size.* Radiat. Prot. Dosim. **52**(1–4), 339–346 (1994).
13. Lunn, D. J., Thomas, A., Best, N. and Spiegelhalter, D. *WinBUGS—a Bayesian modeling framework: concepts, structure, and extensibility.* Stat. Comput. **10**, 325–337 (2000).
14. Nikhoo, H. and Lindborg, L. *RBE of low energy electrons and photons.* Phys. Med. Biol. **55**, R65–R109 (2010).

This page intentionally left blank.

Appendix B

A Comparison of In Vivo Cellular Response to Cs-137 Gamma rays and 320 kV X Rays

The following pages contain the second deliverable provided by LRRI.

Dose-Response (Prepress)
Formerly Nonlinearity in Biology, Toxicology, and Medicine
Copyright © 2013 University of Massachusetts
ISSN: 1559-3258
DOI: 10.2203/dose-response.12-050.Scott

International Dose-Response Society
www.Dose-Response.org

A COMPARISON OF IN VIVO CELLULAR RESPONSES TO CS-137 GAMMA RAYS AND 320-KV X RAYS

B. R. Scott, K. M. Gott □ Lovelace Respiratory Research Institute, Albuquerque, NM

C. A. Potter □ Sandia National Laboratories, Organization 00545, Albuquerque, NM

J. Wilder □ Lovelace Respiratory Research Institute, Albuquerque, NM

□ Research reported here relates to comparing the relative effectiveness of 320-kV X rays compared to Cs-137 gamma rays for two in vivo endpoints in C.B-17 mice after whole-body exposure: (1) cytotoxicity to bone marrow cells and splenocytes evaluated at 24-hours post exposure and (2) bone marrow and spleen reconstitution deficits (repopulation shortfalls) evaluated at 6 weeks post exposure. We show that cytotoxicity dose-response relationships for bone marrow cells and splenocytes are complex, involving negative curvature (decreasing slope as dose increases), presumably implicating a mixed cell population comprised of large numbers of hypersensitive, modestly radiosensitive, and resistant cells. The radiosensitive cells appear to respond with 50% being killed by a dose < 0.5 Gy. The X-ray relative biological effectiveness (RBE), relative to gamma rays, for destroying bone marrow cells in vivo is > 1, while for destroying splenocytes it is < 1. In contrast, dose-response relationships for reconstitution deficits in the bone marrow and spleen of C.B-17 mice at 6 weeks after radiation exposure were of the threshold type with gamma rays being more effective in causing reconstitution deficit.

Keywords: X rays, gamma rays, RBE, cytotoxicity, bone marrow, splenocytes

INTRODUCTION

Self-shielded cesium-137 chloride (^{137}CsCl) irradiators with radioactivity levels in the International Atomic Energy Agency Categories 1 and 2 (i.e., greater than 27 Ci) are widely used in three major applications (NRC 2008): (1) blood sterilization, (2) bio-medical research involving cells in culture and small animals, and (3) calibration. Cesium-137 chloride was selected for the irradiators because of the radiological properties of Cs-137, including its desirable single (662 keV, for unshielded photons) energy, long half-life, relative low cost, and moderate shielding requirements relative to other radionuclides. A report by the National Research Council (NRC 2008) recommended that careful consideration

Address correspondence to Bobby R. Scott, Lovelace Respiratory Research Institute, 2425 Ridgecrest Drive SE, Albuquerque, NM 87108; Phone: 505-348-9470; Fax: 505-348-8567; E-mail: bscott@LRRI.org

be given to the possibility of replacing Cs-137 irradiators with X-ray irradiators for homeland security purposes.

Research reported here relates to possibly replacing ^{137}CsCl irradiators used in radiobiological research involving small animals with an X-RAD 320 Unit (X-ray source [PXINC 2010]) with energies higher than for a typical X-ray irradiator. The objective of the research reported here was to demonstrate the feasibility of achieving the same success in mouse radiobiology studies employing a 320-kV X-ray unit spectrum as has been achieved with higher energy gamma rays from Cs-137. Success would be expected if the X-ray relative effectiveness compared to gamma rays is not a limiting factor for the radiobiological endpoint of interest. The focus of the studies reported here were on (1) bone marrow and spleen cell destruction shortly (24 hours) after irradiating C.B-17 mice (males and females) and (2) on reconstitution deficits in both organs at 6 weeks post exposure of female C.B-17 mice. Reconstitution deficit refers to the repopulation shortfall in the cell count after allowing time for recovery from radiation-induced cell killing (cytotoxicity). *Our emphasis was on determining if the X-Ray relative effectiveness compared to gamma rays was a limiting factor in achieving study success.*

METHODS

Animals

Female and male C.B-17 mice (10 - 18 weeks old) were either bred at Lovelace Respiratory Institute or purchased from Taconic (Germantown, NY). Animals were housed in sterile microisolator caging with autoclaved bedding. They received irradiated food (Teklad Global 18% Protein Rodent Diet 1918 Irradiated, Harlan Laboratories, Madison, WI) and antibiotic treated water (enrofloxacin, 175 mg/mL) (Baytril 100, Bayer HealthCare) for the duration of our studies. For the first 14 days post-irradiation, mice were supplemented with moistened food daily. Lab gel (Banana flavored enrichment gel, no sugar added 71-01-1081, ClearH2O, Portland, ME) was provided as necessary. *All experiments were approved by the Institutional Animal Care and Use Committee* and were conducted at Lovelace Respiratory Research Institute, an AAALAC-approved facility.

Irradiators

Gammacell-1000 Unit

The Gammacell-1000 unit (AECL 1984) used is a self-contained irradiator that was designed to deliver large radiation doses to small biological samples. The irradiator consists of a stationary Cs-137 doubly-encapsulated radiation source permanently secured within a steel-encased, lead biological shield. The biological shield is mounted on a steel frame and covered with sheet-metal panels. The biological shield contains the sam-

ple chamber rotor. By turning the rotor through an arc of up to 180 degrees, the sample chamber is either exposed to or removed (except for leakage radiation) from the radiation field. The radioactive source consists of an array of two ^{137}CsCl pencils (Model ISO-1000; AECL 1984).

X-RAD 320 Unit

The X-RAD 320 Unit (PXINC 2010) is a self-contained X-ray irradiation system that is designed for use in biology and medical research. The X-RAD 320 Irradiation System is used in conjunction with the GE ISOVOLT 320 TITAN X-ray unit. A Cathode Generator with a Power Electronics Module and Anode Generator are used to generate the negative and positive high voltages used to excite the X-ray tube. For our unit, an oil-to-air cooling system is employed.

Animal Irradiation

Just before the first of two dose fractions, mice were anesthetized with 75 – 100 mg/kg ketamine (Putney and/or Fort Dodge Animal Health, Inc) and 5 mg/kg xylazine (Anased, Akorn, Inc.) delivered in a maximum of 0.20 mL saline i.p. Anesthetized mice were placed in 50 mL polypropylene conical centrifuge tubes with the conical end removed to allow a 7 mm hole for breathing. They were secured in the tubes with absorbent wipes placed in front of the tube cap. All radiation doses were delivered as a split dose (i.e., two separate dose fractions) with 50% of the dose being delivered in each of two sessions separated by 4 hours. Between the two irradiation sessions, mice were allowed to wake up from their anesthesia on temperature controlled warming pads and once awake were placed back in their cages with access to food and water. Just before the second dose fraction, mice were again anesthetized with the indicated amount of ketamine and xylazine. No adverse effects were observed related to the two applications of anesthesia.

Tubes were secured horizontally on a turntable in the X-RAD 320 Unit whereas they were positioned vertically in the stainless steel sample canister in the Gammacell 1000 Unit. Mice were rotated on turntables for the duration of the radiation exposures to allow for more uniform distribution of dose. In addition, because the X-ray source was above the mice, the tubes were positioned with the ventral side of the mouse facing the source during the first irradiation session and during the second session the tubes were positioned such that their dorsal side was facing the source. The rotation reduces the risk of damage to the skin.

For our 24-hour study of cytotoxicity to bone marrow and spleen, 21 mice (males and females combined) were used. For our 6-week study of organ reconstitution (recovery/repopulation), data for 13 female mice are reported in this paper. Data for 7 male mice were inconsistent and are excluded.

Dosimetry

Radiation absorbed doses to mice were evaluated using Thermoluminescent Dosimeters (TLD, Quantaflux, Oregonia, OH) which were read on-site using a Victoreen 2800 Thermoluminescent Reader. Dose calibration relationships for the X-RAD 320 unit were established based on Victoreen ionization chamber wands and a Condenser R-Meter Model 570 (Fluke Biomedical, Cleveland, OH). Gammacell 1000 Unit exposure readings based on TLDs were confirmed using nanoDots (Optically Stimulated Luminescence Technology, Landauer, Glenwood, IL). Initial dosimetry was performed by inserting TLDs into mouse carcasses in the inguinal area near femurs to estimate the dose to the bone marrow. These values were used to determine the exposure times for experimental runs. Experimental doses were measured by TLDs taped either to center of turntable (X-RAD 320 Unit) or taped to the outside of exposure tubes (Gammacell 1000 Unit). Gamma-ray doses ranged from 0 to 7.11 Gy. X-ray doses ranged from 0 to 4.74 Gy.

Bone Marrow and Spleen Isolation

Mice were euthanized by i.p. injection of an overdose of Euthasol (0.5 cc 10% Euthasol, Virbac AH, Inc., 300 - 500 mg/kg). Spleen and hind legs were aseptically removed. For bone marrow isolation, femur and tibia bones were isolated and cleaned of muscle and soft tissue. Bones were cut at the ends and the marrow was flushed into 50 ml tubes with complete RPMI (Cellgro) with 5% FBS (Atlanta Biologicals) using a 25 gauge needle and 10 cc syringe.

Splenocytes were isolated by pressing the spleen between frosted ends of sterile microscope slides and collecting cells into 15 mL tubes by rinsing with complete RPMI plus 5% FBS. Bone marrow and spleen cells were spun at 300 x g, for 10 minutes, and resuspended in ACK Lysis Buffer (hypotonic ammonium chloride) to remove RBC. Cells were washed in HBSS and resuspended in complete RPMI with 5% FBS, and filtered through a 40 μm pore size cell strainer (Falcon, BD Biosciences). Cell counts were made under a compound microscope using a hemocytometer and dilutions of Trypan Blue.

Modeling Approaches

An empirical model developed based on exploratory analyses was used for characterizing in vivo cytotoxicity dose-response relationships for bone marrow cells and splenocytes at 24 hours after radiation exposure of C.B-17 mice. A Bayesian approach implemented via Markov chain Monte Carlo was used to obtain model parameter values (Gilks *et al.* 1996; Gamerman 1997; Siva 1998). An Appendix is provided summarizing the Bayesian approach discussed. A separate empirical model, also developed

TABLE 1. In vivo bone marrow cytotoxicity hazard data evaluated at 24 hours after whole-body Cs-137 gamma- or 320-kV X-ray exposure of male and female C.B-17 mice.[a]

X-Ray Data		Gamma-Ray Data	
Dose (Gy)	Observed Hazard	Dose (Gy)	Observed Hazard
0	0	0	0
0	0	0	0
0	0	0	0
1.94	1.17	2.42	1.56
1.94	2.18	2.42	1.47
1.94	1.04	2.42	1.64
3.35	2.06	4.7	1.83
3.35	1.89	4.7	1.48
3.35	1.67	4.7	1.68
4.74	1.89	6.11	2.06
4.74	2.15	6.11	1.69
4.74	1.72	6.11	2.24

[a]Cytotoxicity hazard was evaluated relative to the average number of cells scored in control mice. Data for male and female mice were similar so all the data were used. Each data entry relates to a single animal.

based on exploratory analyses, was used for characterizing reconstitution deficits in bone marrow and spleen at 6 weeks after radiation exposure of C.B-17 mice. Linear regression was used with applying the second model. More details on the modeling conducted are provided in the section titled Results and Discussion and in the Appendix.

RESULTS AND DISCUSSION

Data Used in Modeling

Table 1 shows the in vivo 24-hour post-exposure, bone-marrow cytotoxicity data (cytotoxicity hazard) used in our analyses. Bone marrow data derived from male and female mice were similar as expected and both were used. The cytotoxicity hazard was evaluated as explained in the next section. Table 2 shows the corresponding splenocyte data. Splenocyte data for males and females were similar as expected and both were used. Table 3 shows the week 6, post-exposure bone marrow cellularity data for female C.B-17 mice used in our analyses of cell count deficits. Table 4 shows the corresponding splenocyte cellularity data.

Relative Biological Effectiveness Evaluation

Exploratory analyses of 24-hour, post-exposure splenocyte and bone marrow cell survival (in vivo) data were conducted to help select a plausible model to use for relative biological effectiveness (RBE) evaluation

TABLE 2. In vivo splenocyte cytotoxicity hazard data evaluated at 24 hours after Cs-137 gamma- or 320-kV X-ray exposure of female C.B-17 mice.[a]

X-Ray Data		Gamma-Ray Data	
Dose (Gy)	Observed Hazard	Dose (Gy)	Observed Hazard
0	0	0	0
0	0	0	0
0	0	0	0
1.94	1.68	2.42	2.92
1.94	2.11	2.42	2.66
1.94	1.97	2.42	2.55
3.35	3.07	4.7	4.54
3.35	2.53	4.7	3.39
3.35	2.31	4.7	3.21
4.74	2.92	6.11	3.31
4.74	3.06	6.11	3.64
4.74	3.51	6.11	3.46

[a]Cytotoxicity hazard evaluated relative to the average number of cells scored in control mice. Data for male and female mice were similar so all the data were used. Each data entry relates to a single animal.

TABLE 3. Bone marrow cell counts in female C.B-17 mice and body weights of the mice at 6 weeks after gamma-ray exposure.[a]

Dose (Gy)	Cells (millions)	Weight (g)
0	15.69	23.7
0	15.17	24.8
2.68	17.13	25.2
2.68	15.00	29.5
2.70	22.79	21.9
2.83	20.94	23.1
4.64	15.63	30.1
4.79	14.94	24.7
5.16	10.38	23.8
6.15	9.69	25.2
6.38	14.78	25.6
6.38	14.50	23.0
7.11	8.69	22.1

[a]Each data entry relates to a single animal.

for 320 kV X rays vs. Cs-137 gamma rays. In carrying out the exploratory analyses the surviving fraction data were converted to corresponding cytotoxicity hazard data using the following equation

$$H(D_j) = -\ln[S(D_j)], \tag{1}$$

where $S(D_j)$ is the surviving fraction and $H(D_j)$ is the cytotoxicity hazard as a function of the radiation dose D_j for radiation of type j (X rays or

TABLE 4. Splenocyte counts in female C.B-17 mice and body weights of the mice at 6 weeks after gamma-ray exposure.[a]

Dose (Gy)	Cells (millions)	Weight (g)
0	130.31	23.7
0	161.88	24.8
2.68	155.00	25.2
2.68	130.21	29.5
2.70	177.71	21.9
2.83	156.04	23.1
4.64	142.81	30.1
4.79	127.81	24.7
5.16	90.21	23.8
6.15	82.81	25.2
6.38	69.06	23.0
6.38	127.5	25.6
7.11	84.06	22.1

[a]Each data entry relates to a single animal.

gamma rays). Equation 1 follows from the fundamental relationship between the survival probability and the cumulative hazard function as they relate to all-or-none biological effects (Scott 1984, 1986, 2004). The effect modeled can be cell death, neoplastic transformation, cancer occurrence, organ dysfunction, acute lethality, etc. (Scott 2004). Because of its allowance for a variety of different curve shapes, we used the following empirical model with parameters $D_{50,\mathrm{j}}$ (median effective dose) and v (shape parameter) (Scott 2004):

$$H(D_{\mathrm{j}}) = [\ln(2)][D_{\mathrm{j}}/D_{50,\mathrm{j}}]^{v}. \tag{2}$$

For $v = 1$, a linear no-threshold (LNT) relationship arises for the cytotoxicity hazard. For $v = 2$, a quadratic relationship (i.e., positive curvature, with the slope progressively increasing as dose increases) arises. Linear (no curvature) and positive curvature dose-response relationships are typical for *in vitro* studies of cell survival after exposure to low-LET photon radiation when the surviving fraction is plotted using a logarithmic scale and dose is plotted using a linear scale (Scott 1977; Fertil *et al.* 1984; Fertil and Malaise 1985). For $v < 1$, negative curvature (i.e., decreasing slope with increasing dose) arises which is unusual for *in vitro* studies of homogeneous populations exposed to low-LET photon radiation but appears to be the case for our *in vivo* data presented here which can be presumed to be explained on the basis of a heterogeneous population. For ionizing photon radiation, the shape parameter v is expected to be independent of the type of radiation (Scott 2004), which was assumed here.

We used the Bayesian approach, implemented via Markov chain Monte Carlo (MCMC, Lunn *et al.* 2000), to estimate model parameters

TABLE 5. Summary of MCMC results obtained for splenocytes and bone marrow cells evaluated in vivo after whole-body exposure of male and female C.B-17 mice to Cs-137 gamma rays or 320-kV X rays.

Cells	Parameter	mean	sd	5%	10%	50%	90%	95%
Splenocytes	$D_{50,g}$ in Gy	0.0871	0.040	0.0326	0.0399	0.0818	0.141	0.161
Splenocytes	$D_{50,x}$ in Gy	0.112	0.043	0.05	0.0593	0.107	0.169	0.19
Splenocytes	v	0.382	0.044	0.311	0.324	0.381	0.439	0.456
Splenocytes	RBE[a]	0.763	0.109	0.583	0.623	0.763	0.902	0.943
Bone marrow	$D_{50,g}$ in Gy	0.17	0.077	0.0681	0.0811	0.158	0.276	0.32
Bone marrow	$D_{50,x}$ in Gy	0.134	0.072	0.0444	0.0553	0.121	0.233	0.277
Bone marrow	v	0.288	0.045	0.223	0.233	0.284	0.348	0.370
Bone marrow	RBE[a]	1.346	0.283	0.965	1.026	1.305	1.709	1.862

[a] RBE values refer to X rays relative to gamma rays.

D_{50} and v (see Appendix for more details). The cytotoxicity hazard $H(D_j)$ was modeled as being normally distributed for a given value of D_j with a standard deviation equal to the standard deviation for the experimental data fitted with the model. With this approach, one obtains not only a posterior distribution mean (central estimate) for a given parameter but also the standard deviation and percentiles (e.g., 5%, 10%, 50%, 90%, 95%) of the posterior distribution. The prior distribution used for $D_{50,j}$ for splenocytes was uniform from 0.01 to 5.0 Gy. For bone marrow cells, the corresponding distribution was uniform from 0.01 to 2.0 Gy. For both cell types, the prior distribution used for v was uniform from 0.05 to 1.0, because of negative curvature in the dose-response data revealed by exploratory analysis.

The 320 kV X-ray and Cs-137 gamma-ray data for a given cell type were simultaneously fit to facilitate evaluating a common value for the parameter v. One hundred thousand iterations (single chain) were used for the MCMC analysis for bone marrow cells and 140 thousands iterations for splenocytes, with only the last 20,000 results retained for each cell type for analysis. The number of iterations and data discarding were based on autocorrelations observed over the first 5000 iterations. The discarded MCMC-generated data represents what is called *burn-in* (see Appendix for more discussion).

The X-ray RBE for in vivo cytotoxicity relative to gamma rays was evaluated based on the following equation:

$$\mathrm{RBE} = D_{50,g}/D_{50,x}. \tag{3}$$

Because $D_{50,g}$ and $D_{50,x}$ have posterior distributions, RBE also has a posterior distribution. We used the mean of the posterior distribution as our central estimate of RBE.

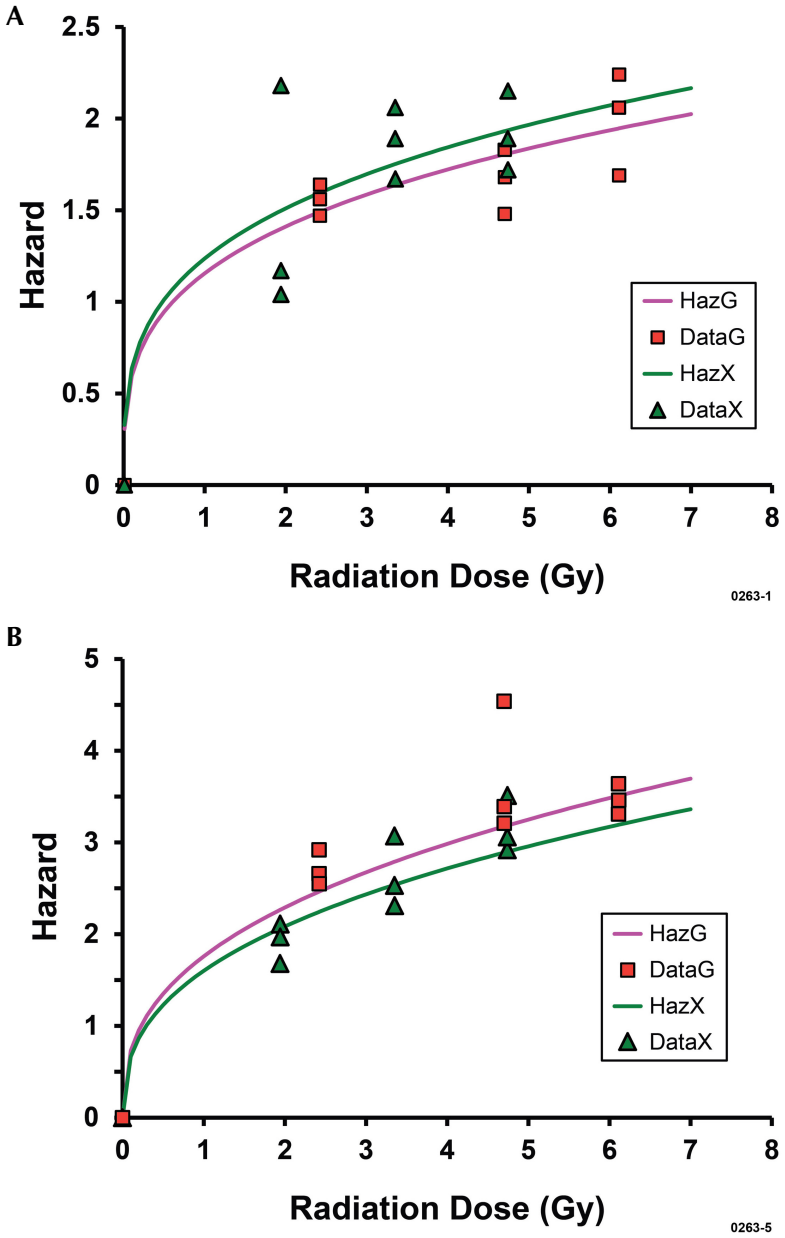

FIGURE 1A. Cytotoxicity hazard for bone marrow cells in vivo at 24 hours after X-ray or gamma-ray exposure of C.B-17 mice (combined data for males and females): HazG, fitted line for gamma rays; DataG, gamma-ray data; HazX, fitted line for X rays; DataX, X-ray data. **FIGURE 1B.** Corresponding results for splenocytes: HazG, fitted line for gamma rays; DataG, gamma-ray data; HazX, fitted line for X rays; DataX, X-ray data.

Table 5 and Figures 1A and 1B show results (cytotoxicity hazards) obtained in our MCMC analyses of data for early-on (24-hours after exposure) cytotoxicity for the two cell and two radiation types. Negative-curvature, dose-response relationships were observed for both X rays and gamma rays and for both cell types and *implicate heterogeneous (mixed) cell*

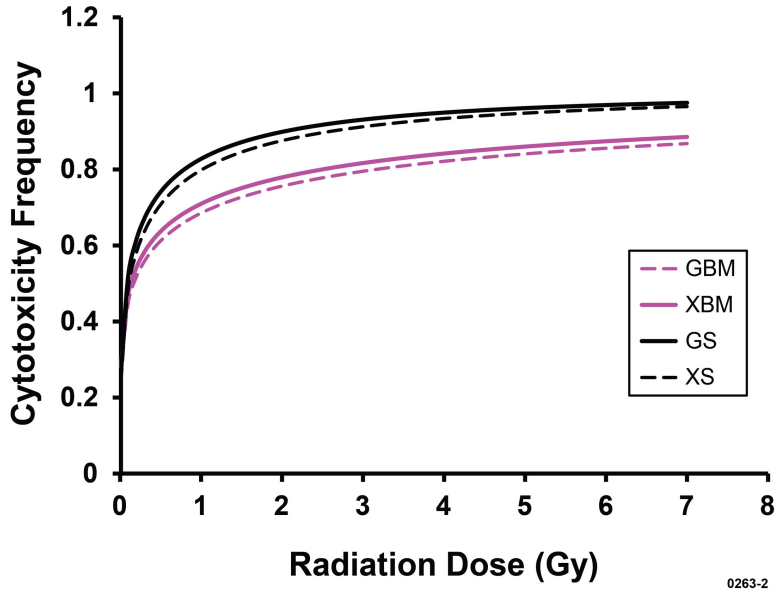

FIGURE 2. Central estimates of the frequency of cytotoxicity (cell killing) to bone marrow cells and splenocytes in vivo for X-ray and gamma-ray exposure of female C.B-17 mice based on curves presented in Figures 1A and 1B. GBM, for gamma rays and bone marrow; XBM, for X rays and bone marrow; GS, for gamma rays and splenocytes; XS, for X rays and splenocytes.

populations as is known to be the case. While the doses $D_{50,x}$ and $D_{50,g}$ for killing 50% of the target cells were < 0.5 Gy, the added dose needed to kill the remaining 50% of the cells exceeded 6 Gy. Thus, a large number of cells in the target populations appear to be radiosensitive, a large number appear modestly radiosensitive, and a large number appear quite resistant to being killed.

X rays were found to be more effective (RBE = 1.35, posterior distribution mean) than gamma rays in damaging bone marrow cells inside the body. In contrast, X rays were found to be less effective (RBE = 0.76, posterior distribution mean) than gamma rays in damaging splenocytes inside the body. Similar estimates of RBE can also be obtained based on the separate posterior distribution means for $D_{50,g}$ and $D_{50,x}$ presented in Table 5. Figure 2 shows the corresponding dose-response relationships for the cytotoxicity frequency (i.e., cell killing frequency) which was evaluated as $1 - S(D_j)$, where based on Equation 1,

$$S(D_j) = \exp[-H(D_j)]. \tag{4}$$

Exploratory-Analysis-Based Equations for Evaluating Reconstitution Deficit

Data in Tables 3 and 4 were first evaluated for correlations between key variables (D_j, $C(D_j)$, and body weight). Because $C(D_j)$ might be influ-

TABLE 6. Results of correlation analyses related to bone marrow and spleen cellularity at 6 weeks after whole-body exposure of female C.B-17 mice to gamma or X rays

Radiation Type	Tissue	Comparison	Correlation Coefficient	Degrees of Freedom	Significance (p value)
Gamma	Bone marrow	Cell count vs. weight	–0.075	11	> 0.5
Gamma	Bone marrow	Cell count vs. dose	–0.54	11	< 0.05[a]
Gamma	Spleen	Cell count vs. weight	0.145	11	> 0.5
Gamma	Spleen	Cell count vs. dose	–0.712	11	< 0.01[a]
X rays	Bone marrow	Cell count vs. weight	0.03	12	> 0.5
X rays	Bone marrow	Cell count vs. dose	0.19	12	> 0.5[b]
X rays	Spleen	Cell count vs. weight	0.377	12	> 0.1
X rays	Spleen	Cell count vs. dose	–0.296	12	> 0.2[b]

[a]Results implicate an increasing deficit in cellularity as the gamma-ray dose increases.
[b]Results implicate no deficit in the cellularity irrespective of dose.

enced by organ weight, data for $C(D_j)$ in millions of cells were first evaluated against body weight in grams. This approach is based on the assumption that at the end of a fixed follow-up time, organ weight and body weight are correlated for animals of similar ages. For the female C.B-17 mice studied and related ages, no significant correlations were observed ($p > 0.05$) as indicated in Table 6. In contrast, significant correlations were found when data for $C(D_j)$ were evaluated against the gamma-ray dose D_g but not when evaluated against the X-ray dose D_x (for the lower dose range studied for X rays based on a study design RBE of 1.3), as indicated in Table 6. This along with other results from data exploratory analyses was interpreted to indicate that cell reconstitution deficit increases with gamma-ray dose above the threshold (i.e., for the excess dose $D - T$) but not for X-ray exposure over the dose-range studied (implicating $T >$ maximum D_x used). Thus, our analyses revealed that Cs-137 gamma rays appear to be more effective (lower threshold T) than 320-kV X rays in causing reconstitution deficit at 6 weeks after radiation exposure. Full reconstitution is implicated after the X-ray doses used. These observations are consistent with the splenocyte cytotoxicity hazard data in Figure 1B (X-ray RBE = 0.76) but not the bone marrow cytotoxicity data in Figure 1A (X-ray RBE = 1.3).

Additional exploratory analyses of bone marrow and spleen cellularity (cell counts) at 6 weeks after gamma-ray exposure of female C.B-17 mice were conducted to provide guidance on a plausible dose-response model. In the analysis, dose-response relationships were expressed using log vs. linear, linear vs. log, and log vs. log scales. These analyses revealed two components to the dose-response relationship for the cell count: (1) a low-dose range where cellularity was the same as for controls; (2) a high-dose range where there was a deficit in the cell count relative to controls (i.e., reconstitution deficit) and the cell count decreased exponentially as

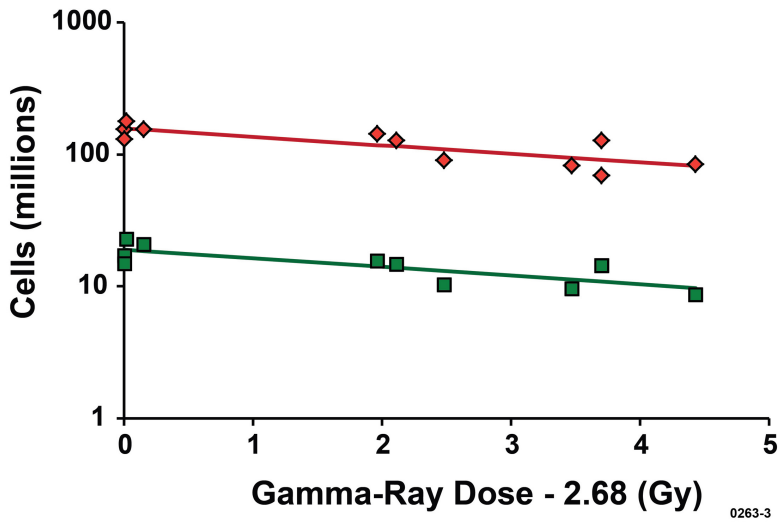

FIGURE 3. Dose-response relationships for bone marrow (lower line) and spleen (upper line) cellularity for female C.B-17 mice exposed to gamma rays 6 weeks prior to animal sacrifices. The upper line has the intercept N_0 = 157 million cells. The lower line has the intercept N_0 = 19 million cells. These values for N_0 were used to obtain results presented in Figure 4.

dose increased above a threshold dose T for a deficit. The low dose range comprised only two doses (controls and lowest non-zero dose group). Based on the indicated observations, the following model was used to characterize the expected cell count $C(D)$ (in millions) in spleen and bone marrow of C.B-17 mice as a function of the radiation dose D that was received 6 weeks earlier:

$$C(D) = N_0, \text{ for } D < T.$$

Otherwise,

$$C(D) = N_0 \exp[-\alpha\ (D - T)]. \tag{5}$$

The threshold T was estimated as the largest dose applied that was not associated with a deficit in the cell count at 6 weeks after radiation exposure. This however corresponded to the lowest non-zero dose group as already indicated. The reconstitution deficit, $deficit(D)$, of the cell count in millions was evaluated based on the following relationships:

$$deficit(D) = 0, \text{ when } D < T.$$

Otherwise,

$$deficit(D) = N_0 - C(D) = N_0(1 - \exp[-\alpha(D - T)]). \tag{6}$$

TABLE 7. Results of regression of data for $\ln[C(D_g)]$ vs. "$D_g - 2.68$", for $D_g \geq 2.68$ Gy, for bone marrow cells and splenocytes at 6 weeks after whole-body, gamma-ray exposure of female C.B-17 mice.

Parameter	Tissue	Parameter Value and Standard Error
$\ln[N_0]$	Bone marrow	2.933 ± 0.098 [a]
$\ln[N_0]$	Spleen	5.056 ± 0.093[b]
α (Gy^{-1})	Bone marrow	0.134 ± 0.038
α (Gy^{-1})	Spleen	0.15 ± 0.04[c]

[a]$N_0 = \exp(2.933) = 19$ million cells (rounded).
[b]$N_0 = \exp(5.056) = 157$ million cells (rounded).
[c]Not significantly different from bone marrow, $p > 0.3$.

Model parameter N_0 and α were estimated based on linear regression of data for $\ln[C(D)]$ against the excess dose "$D - T$" for doses $D \geq T$. With this approach, the intercept obtained is an estimate of $\ln[N_0]$ and the slope multiplied by –1 is an estimate of α. N_0 is then evaluated by exponentiation of the estimate obtained for $\ln[N_0]$.

Dose-Response Relationships for $C(D_j)$ and *deficit*(D_j)

Dose-response relationships for $C(D_j)$ are presented in Figure 3 for both bone marrow cells and splenocytes with T estimated to be 2.68 Gy. Data for $C(D_j)$ are plotted against the excess dose $(D - T)$ for $D \geq 2.68$ Gy. $C(D)$ (cells in millions) is plotted on a logarithmic scale against the excess dose "$D - 2.68$" Gy on a linear scale. The slope parameter α was not significantly different ($p > 0.3$) for bone marrow cells and splenocytes (see Table 7 for values). The intercept N_0 for splenocytes was 157 million cells (rounded central estimate) and for bone marrow cells the rounded central estimate was 19 million cells (see footnotes *a* and *b* for Table 7).

The indicated central estimates of N_0 were used to evaluate *deficit*(D_g) for both bone marrow cells and splenocytes at 6 weeks after Cs-137 gamma-ray exposure of female C.B-17 mice. Results obtained are presented in Figure 4 as a function of the excess dose, for $D_g \geq 2.68$ Gy. Much larger reconstitution deficits were revealed for splenocytes compared to bone marrow cells. For a given dose D_g, *deficit*(D_g) was a factor of 157/19 = 8.3 larger (central estimate) for splenocytes than for bone marrow cells. This was not the case for X rays for which the data for $C(D_x)$ did not reveal any significant negative correlations of $C(D_x)$ with dose D_x for the more limited range of doses studied for both bone marrow cells and splenocytes (Table 6). We interpret this to mean that T for X-ray exposure is larger and/or α is much smaller than for gamma-ray exposure. If so, larger X-ray doses would be needed to demonstrate a reconstitution deficit in bone marrow cells and splenocytes at 6 weeks after radiation exposure of

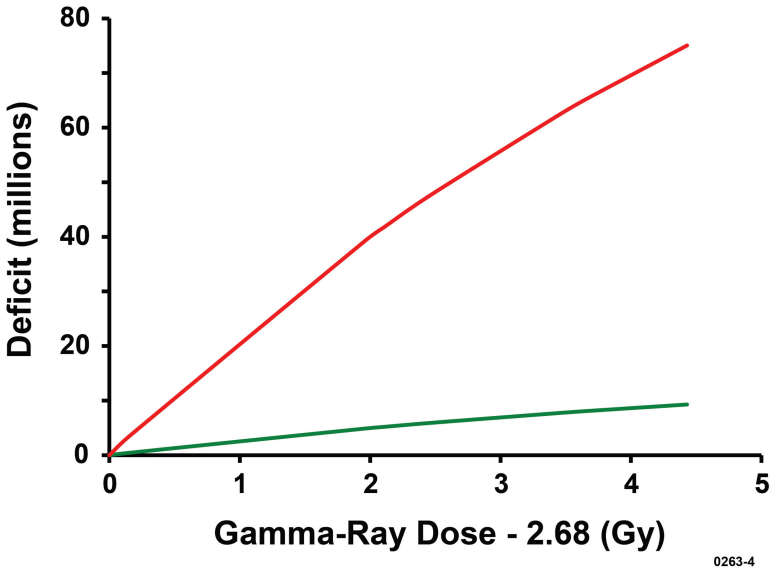

FIGURE 4. Central estimates of reconstitution deficits for splenocyte (upper red curve) and bone marrow cells (lower curve) in female C.B-17 mice at 6 weeks after exposure to gamma rays. No deficits were found for mice exposed to X rays for the shorter range of doses used for X rays (data not presented).

female C.B-17 mice. Larger X-ray doses than used in our studies may be needed for successful bone marrow transplantation studies using 320-kV X rays or lower energy X rays (Scott *et al.* 2012).

CONCLUSIONS

Early (24-hour, post-exposure) in vivo cytotoxicity dose-response relationships for bone marrow cells and splenocytes of C.B-17 mice are complex, showing negative curvature, implicating a mixed cell population comprised of large numbers of hypersensitive, modestly radiosensitive, and resistant cells. The radiosensitive cells appear to respond without a threshold radiation dose, however additional studies are needed to confirm this. Modest and high doses of both Cs-137 gamma rays and 320-kV X rays can destroy large numbers of both bone marrow cells and splenocytes of C.B-17 mice. The X-ray RBE relative to gamma rays for destroying bone marrow cells in vivo is > 1 while for destroying splenocytes is < 1. In contrast, dose-response relationships for reconstitution deficits in the bone marrow and spleen of C.B-17 mice at 6 weeks after radiation exposure were of the threshold type with gamma rays being more effective (lower threshold) in causing reconstitution deficits in both the bone marrow and spleen. It is important to consider these reconstitution deficit differences for Cs-137 gamma-ray and 320-kV X-ray exposures when designing mouse bone marrow transplantation studies using 320-kV X rays.

ACKNOWLEDGEMENTS

This work was performed under project number SL11-RadBio-PD13 and with partial support from the Office of Science (BER), U.S. Department of Energy, Grant No. DE-FG02-09ER64783. The authors would like to express their appreciation to the U. S. Department of Energy, NA-22, Radiation Source Replacement Program and Frances Keel (DOE/NA-221). We are also grateful to Susan Longley of Sandia National Laboratories who had a major role in the acquisition and initiation of this project and to the reviewers of the paper.

APPENDIX

Estimating Cytotoxicity Model Parameters using Bayesian Inference Implemented with MCMC

With the Bayesian approach, model parameters and the biological effects for data of interest (e.g., cytotoxicity hazard) are considered random variables (Gamerman 1997; Siva, 1998). If "**data**" is used to denote the observed *biological effects vector* and $\boldsymbol{\theta}$ is used to denote a *model parameters vector*, then formal Bayesian inference requires setting up a *joint probability distribution* $P(\mathbf{data},\boldsymbol{\theta})$ over the quantities in the two vectors (biological effects and model parameters). This joint distribution comprises two parts: a prior distribution, $P(\boldsymbol{\theta})$, and a likelihood, $P(\mathbf{data}|\boldsymbol{\theta})$. The vertical bar indicates that the data vector is conditional on the parameter vector $\boldsymbol{\theta}$. The joint probability distribution is specified as

$$P(\mathbf{data},\boldsymbol{\theta}) = P(\mathbf{data}|\boldsymbol{\theta})P(\boldsymbol{\theta}) = P(\boldsymbol{\theta}|\mathbf{data})P(\mathbf{data}). \tag{A1}$$

Both $P(\boldsymbol{\theta})$ and $P(\mathbf{data})$ are unconditional distributions. When new observations are available, Bayes theorem is used to update the distribution of the parameters $P(\boldsymbol{\theta}|\mathbf{data})$ given (i.e., conditional on) the new data. The Bayesian updating relationship can be expressed as (Siva, 1998):

$$P(\boldsymbol{\theta}|\mathbf{data}) = P(\mathbf{data}|\boldsymbol{\theta})P(\boldsymbol{\theta}) \;/\int P(\mathbf{data}|\boldsymbol{\theta})P(\boldsymbol{\theta})\,d\boldsymbol{\theta} = P(\mathbf{data}|\boldsymbol{\theta})P(\boldsymbol{\theta})/\mathrm{P}(\mathbf{data}). \tag{A2}$$

Depending on the complexities of the model being addressed, analytical solutions to Equation A2 may exist. Analytical solutions do not exist for many complex stochastic models. However, whether or not an analytical solution exists, the integral can be estimated numerically using MCMC (Gilks *et al.* 1996; Lunn *et al.* 2000).

MCMC methods are a group of sophisticated methods that are often used in complex Bayesian analyses. The most common implementation uses what are called the Metropolis-Hastings algorithm and Gibbs sampling. Markov chains provide a framework under which simulation tech-

niques may be used to explore various distribution properties, generally focused on the posterior distribution. Gibbs sampling is iterative and allows the marginal distribution of model parameters (e.g., v, $D_{50,g}$, $D_{50,x}$) to be directly sampled. The Markov chain component of Gibbs sampling provides the framework from which the random samples are generated. However, it is required that the distribution of all parameters, conditional on all other influential parameters and the data fitted, to be specified to allow Monte Carlo sampling. Generally, single or multiple chains are used and *data from the initial portion from a Markov chain sample is discarded so that the effect of the initial values on the posterior inference is minimized.* The discarded data are called burn-in.

REFERENCES

Atomic Energy of Canada Limited (AECL). 1984. Gammacell 1000 Operator's Manual for Serial Numbers 37 and Up, Edition 3, Technical Publications Document No. IN-J1100-83-04A

Fertil B, Dertinger H, Courdi A, and Malaise EP. 1984. Mean inactivation dose: a useful concept for intercomparison of human cell survival curves. Radiation Research 99(1):73–84

Fertil B, Malaise EP. 1985. Intrinsic radiosensitivity of human cell lines is correlated with radioresponsiveness of human tumors: Analysis of 101 published survival curves. International Journal of Radiation Oncology Biology Physics 11(9):1699-1707

Gamerman D. 1997. Markov Chain Monte Carlo. Stochastic Simulation for Bayesian Inference, Chapman & Hall, London

Gilks WR, Richardson S, Spiegelhalter DJ (editors). 1996. Markov Chain Monte Carlo in Practice, Chapman & Hall, London

Lunn D J, Thomas A, Best N and Spiegelhalter D. 2000. WinBUGS–a Bayesian modeling framework: concepts, structure, and extensibility. Statistics and Computing 10:325–337

National Research Council (NRC). 2008. Radiation Source Use and Replacement. The National Academies Press, Washington, DC

Precision X-Ray, Inc. (PXINC). 2010. X-RAD 320 Users Manual, Document Number: X-RAD320UM-UG, Precision X-Ray, Inc., N. Branford, CT

Scott BR. 1977. Mechanistic state vector model for cell killing by ionizing radiation. Radiation and Environmental Biophysics 14: 195-211

Scott BR. 1984. Methodologies for predicting the expected combined stochastic radiobiological effects of different ionizing radiations and some applications. Radiat Res 98:182-197

Scott BR. 1986. Predictive models for potentiation of cell killing by combined exposure in vitro to photon radiation and BCNU. Mathematical Modeling 7:1339-1352

Scott BR. 2004. Health risks from high-level radiation exposure from radiological weapons. Radiation Protection Management 21(6):9-25

Scott BR, Lin Y, Wilder JA, Hutt JA, Padilla MT, and Gott KM. 2012. Radiobiological Studies using Gamma and X Rays. Project Final Report Contribution. Report provided to Sandia National Laboratories, August 24, 2012.

Siva DS. 1998. Data Analysis, a Bayesian Tutorial. Oxford University Press, New York

DISTRIBUTION:

1 Julie A. Hutt
Lovelace Respiratory Research Institute
2425 Ridgecrest Drive SE
Albuquerque, NM 87108

1 Katherine M. Gott
Lovelace Respiratory Research Institute
2425 Ridgecrest Drive SE
Albuquerque, NM 87108

1 Yong Lin
Lovelace Respiratory Research Institute
2425 Ridgecrest Drive SE
Albuquerque, NM 87108

1 Mabel T. Padilla
Lovelace Respiratory Research Institute
2425 Ridgecrest Drive SE
Albuquerque, NM 87108

1 Bobby R. Scott
Lovelace Respiratory Research Institute
2425 Ridgecrest Drive SE
Albuquerque, NM 87108

1 Julie A. Wilder
Lovelace Respiratory Research Institute
2425 Ridgecrest Drive SE
Albuquerque, NM 87108

1	MS 0425	C. A. Potter, 245
1	MS 0425	S. W. Longley, 249
1	MS 0899	Technical Library, 9536 (electronic copy)

Sandia National Laboratories